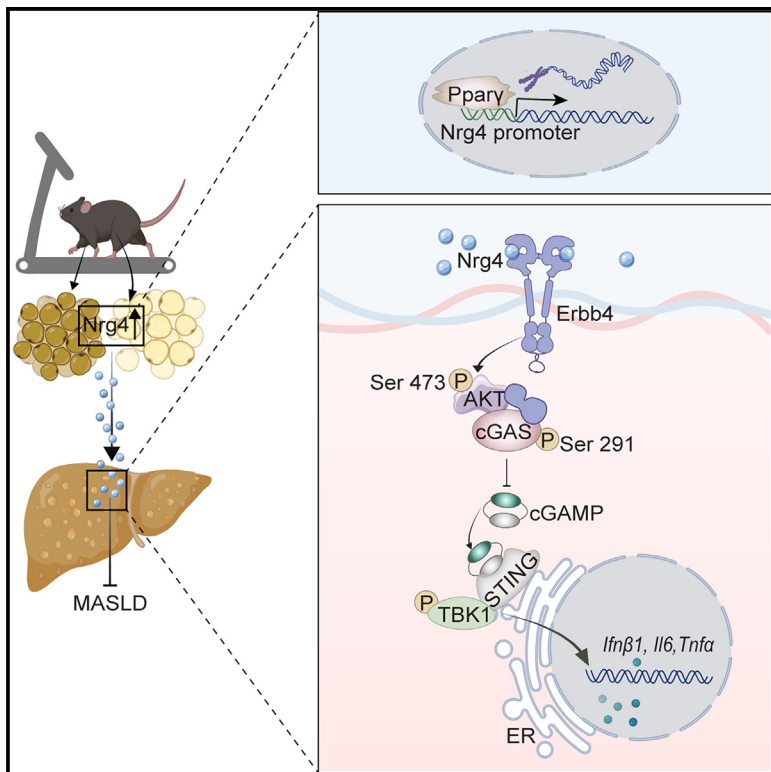


Exercise-induced adipokine Nrg4 alleviates MASLD by disrupting hepatic cGAS-STING signaling

Graphical abstract



Authors

Min Chen, Yang Li, Jie-Ying Zhu, ..., Xin Li, Hu-Min Chen, Liang Guo

Correspondence

guoliang@sus.edu.cn

In brief

Chen et al. show that Nrg4 is an exercise-induced adipokine via Ppary-triggered transactivation and facilitates exercise-mediated alleviation of MASLD, in which Nrg4/Erbb4/AKT axis-mediated inhibition of hepatic cGAS-STING signaling by phosphorylating cGAS is involved. Adipose Nrg4 acts as a downstream effector of exercise to combat MASLD.

Highlights

- Adipose Nrg4 is induced by exercise via Ppary
- Knockdown of adipose Nrg4 impairs exercise-mediated alleviation of MASLD
- Overexpression of adipose Nrg4 relieves MASLD in synergy with exercise
- Nrg4/Erbb4/AKT disrupt hepatic cGAS-STING signaling by phosphorylating cGAS



Article

Exercise-induced adipokine Nrg4 alleviates MASLD by disrupting hepatic cGAS-STING signaling

Min Chen,^{1,2,3} Yang Li,^{1,2,3} Jie-Ying Zhu,^{1,2,3} Wang-Jing Mu,^{1,2,3} Hong-Yang Luo,^{1,2,3} Lin-Jing Yan,^{1,2,3} Shan Li,^{1,2,3} Ruo-Ying Li,^{1,2,3} Meng-Ting Yin,^{1,2,3} Xin Li,^{1,2,3} Hu-Min Chen,^{1,2,3} and Liang Guo^{1,2,3,4,*}

¹School of Exercise and Health and Collaborative Innovation Center for Sports and Public Health, Shanghai University of Sport, Shanghai 200438, China

²Shanghai Frontiers Science Research Base of Exercise and Metabolic Health, Shanghai University of Sport, Shanghai 200438, China

³Key Laboratory of Exercise and Health Sciences of the Ministry of Education, Shanghai University of Sport, Shanghai 200438, China

⁴Lead contact

*Correspondence: guoliang@sus.edu.cn

<https://doi.org/10.1016/j.celrep.2025.115251>

SUMMARY

Exercise is an effective non-pharmacological strategy for ameliorating metabolic dysfunction-associated steatotic liver disease (MASLD). Neuregulin-4 (Nrg4) is an adipokine with a potential role in metabolic homeostasis. Previous findings have shown that Nrg4 is upregulated by exercise and that Nrg4 reduces hepatic steatosis, but the underlying mechanism is not fully understood. Here, we show that adipose Nrg4 is trans-activated by Ppary in response to exercise in mice. Adeno-associated virus (AAV)-mediated knockdown of adipose Nrg4 as well as hepatocyte-specific knockout of Erbb4 (Nrg4 receptor) impair exercise-mediated alleviation of MASLD in mice. Conversely, AAV-mediated overexpression of adipose Nrg4 mitigates MASLD in mice in synergy with exercise. Mechanistically, Nrg4/Erbb4/AKT signaling promotes cyclic guanosine monophosphate-AMP synthase (cGAS) phosphorylation to blunt its enzyme activity, thereby inhibiting cGAS-STING pathway-mediated inflammation and steatosis in hepatocytes. Thus, Nrg4 functions as an exercise-induced adipokine that participates in adipose-liver tissue communication to counteract MASLD.

INTRODUCTION

Exercise is an effective way to prevent metabolic disease, and it exerts its protective effects by improving the metabolic phenotypes of multiple tissues.^{1–4} These multi-tissue adaptations occur not only through exercise-triggered intrinsic signaling events in each tissue but also through exercise-induced integration of inter-tissue communication by a variety of signaling molecules, hormones, and cytokines.^{5,6} Excessive intrahepatic fat storage (hepatic steatosis) is the entryway to metabolic dysfunction-associated steatotic liver disease (MASLD), an umbrella condition that also encompasses steatohepatitis, fibrosis, and cirrhosis.^{7–10} Regular exercise can reduce the risk of developing MASLD.^{11–14} However, the molecular mechanism of how exercise mitigates MASLD remains to be further explored.

Neuregulin 4 (Nrg4) has emerged as an adipose tissue-enriched endocrine factor that can act on multiple tissues, such as the liver, heart, kidney, cartilage, and blood vessels, exerting beneficial effects on tissue metabolic homeostasis.¹⁵ Nrg4 expression is markedly downregulated in mice and humans with MASLD.^{16,17} Interestingly, population studies have shown that a variety of exercises (including moderate-intensity continuous training, circuit resistance training, and high-intensity interval training) can significantly increase the content of Nrg4 in the circulation.¹⁸ Therefore, we speculated that Nrg4 may act as a potential crosstalk factor of exercise between adipose tissue

and the liver that may contribute to exercise-mediated amelioration of MASLD, which was investigated in our present study.

Our previous loss- and gain-of-function experiment in mice showed that Nrg4 suppressed the mRNA expression of genes involved in hepatic inflammation in the progression of nonalcoholic steatohepatitis.¹⁹ A previous report has shown that high circulating levels of Nrg4 suppress chronic inflammation in epididymal white adipose tissue (eWAT).²⁰ Also, another study has shown that brown adipose tissue (BAT)-specific Nrg4 restoration alleviates vascular inflammation in male mice with atherosclerosis,²¹ indicating that Nrg4 has an anti-inflammatory role. However, it is still unclear whether the adipokine Nrg4 can protect against MASLD directly through its anti-inflammatory effect. Cyclic guanosine monophosphate (GMP)-AMP synthase (cGAS)-simulator of interferon genes (STING) signaling is involved in multiple liver diseases, including MASLD,²² liver injury, hepatocellular carcinoma (HCC),²³ and viral hepatitis.²⁴ In patients with MASLD, hepatic STING expression has been demonstrated to be upregulated.^{22,25} The activated STING pathway has been reported to activate the downstream signaling cascades and to promote hepatocyte injury and dysfunction in hepatocytes.²⁶ Furthermore, the cGAS-STING axis is involved in the activation of apoptotic pathways in MASLD, upregulates inflammatory pathways, and induces glucose and lipid metabolism disorders.^{25,27} Although several studies have provided evidence showing that STING is a key factor in promoting the



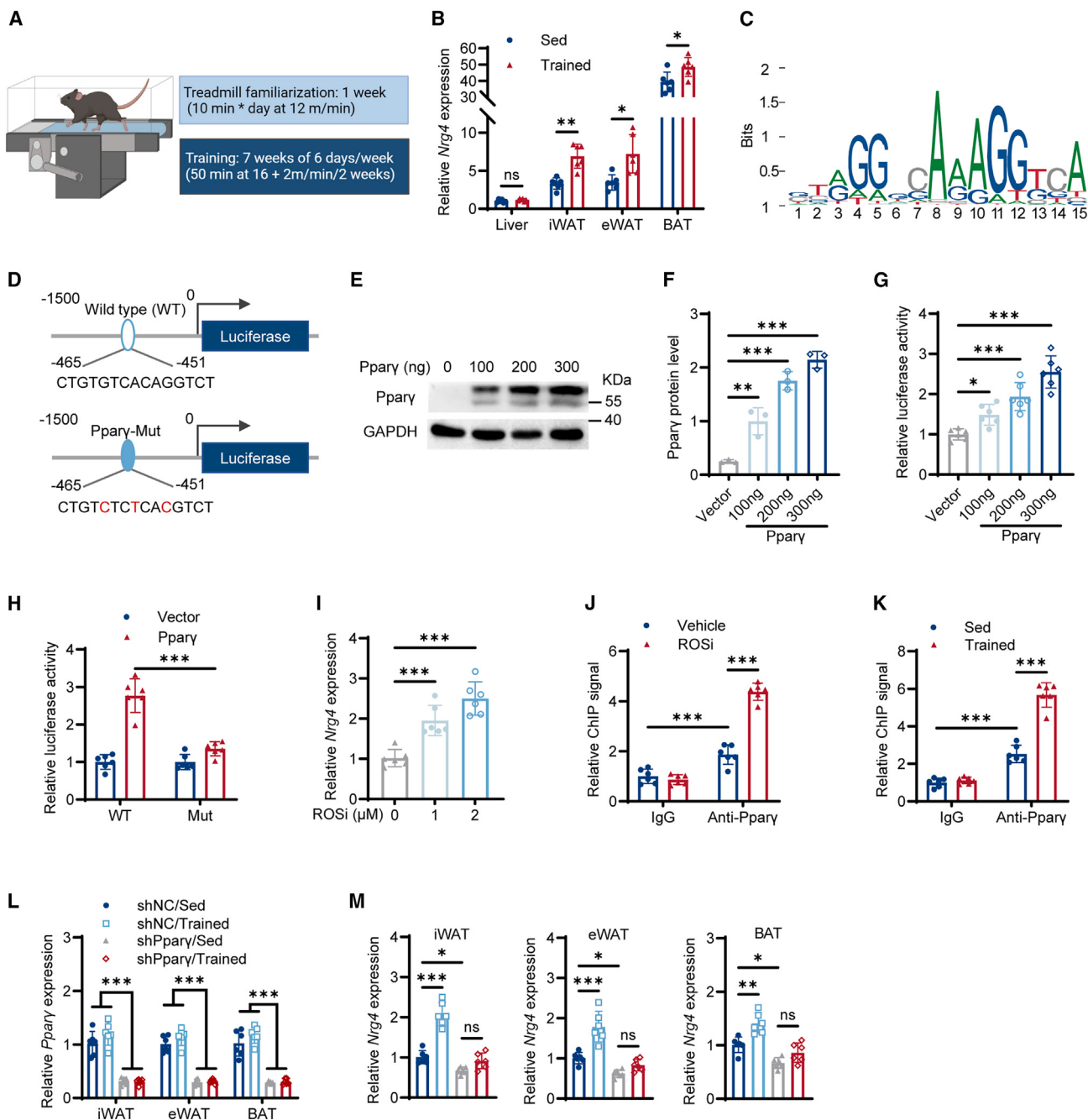


Figure 1. Adipose *Nrg4* is induced by *Ppary* during exercise in mice

(A) Treadmill training in CD-fed 8-week-old male mice. The figure was created using BioRender.

(B) Adipose tissue and liver samples were isolated from male mice after the exercise program shown in (A) was done. The relative mRNA level of *Nrg4* in mouse liver and adipose tissue is shown. iWAT, inguinal white adipose tissue; eWAT, epididymal white adipose tissue; BAT, brown adipose tissue; Sed, sedentary condition; Trained, exercise training condition. Data were normalized to the liver tissue of the Sed group.

(C) The consensus DNA binding sequence of *Ppary*.

(D) Schematic of *Nrg4* proximal promoter constructs used for luciferase assays. The predicted consensus of the *Ppary* binding site is shown in the WT luciferase construct. The red letters indicate mutation (Mut) of the *Ppary* binding site in the mutated construct.

(E–G) HEK293T cells were transiently transfected with the WT (wild-type) reporter construct as shown in (D), along with different amounts of the *Ppary* expression vector.

(E) Western blot of the HEK293T cells lysates.

(F) Quantification of the western blot results in (E) ($n = 3$ independent biological replicates/group).

(G) Luciferase activities were measured.

(legend continued on next page)

MASLD process, it is still important to determine the molecular events underlying the activation of the STING during MASLD. Here, we discover that exercise training increases Nrg4 mRNA expression in mouse adipose tissues. Nrg4 is found to be an exercise-induced adipokine that improves high-fat diet (HFD)-induced hepatic inflammation and steatosis in the mouse liver. Mechanistically, exercise increases Nrg4 expression in adipose tissue by peroxisome proliferator-activated receptor gamma (Ppary)-mediated transactivation, and Nrg4 disrupts cGAS-STING signaling in hepatocytes via Nrg4/ErbB4/protein kinase B (AKT)-mediated phosphorylation of cGAS. This study reveals a significant mechanism by which Nrg4, as an exerkine, contributes to exercise-mediated adipose-liver tissue crosstalk in the fight against MASLD.

RESULTS

Exercise leads to upregulation of adipose Nrg4 expression in a Ppary-dependent manner

To investigate the effect of exercise on Nrg4 expression, wild-type C57BL/6 mice fed a chow diet (CD) were subjected to an established protocol of aerobic exercise (treadmill training) for 8 weeks (Figure 1A). It was found that the expression of Nrg4 in adipose tissue, but not in liver, can be significantly upregulated after exercise (Figure 1B). Previous studies demonstrated that exercise training robustly activated Ppary in both rodents and humans.^{28,29} *In silico* analysis found that the proximal murine Nrg4 promoter contains a putative PPAR-responsive element (PPRE) approximately located at -465 to 451 bp relative to the transcription start site (Figures 1C and 1D). To determine whether the potential PPRE mediates the induction of Nrg4 by Ppary, we constructed the luciferase reporters driven by the murine wild-type (WT) Nrg4 promoter, or mutated promoters, in which three core sites within the predicted PPRE were mutated (Figure 1D). Our results showed that Ppary enhanced the luciferase activity in a dose-dependent manner (Figures 1E–1G). Mutation analysis showed that mutating the core sites of PPRE in the Nrg4 promoter abolished Ppary-mediated activation of the Nrg4 promoters (Figure 1H). Furthermore, our results showed that the mRNA level of Nrg4 was significantly elevated after intervention with the Ppary agonist rosiglitazone (Rosi) in 3T3-L1 adipocytes (Figure 1I). Our chromatin immunoprecipitation data revealed that Ppary can bind to the promoter of Nrg4 in adipocytes and that the binding to the Nrg4 promoter is enhanced after treatment with Rosi (Figure 1J). Consistent with the *In vitro* results, treadmill exercise for 8 weeks enhanced the binding level

of Ppary to the promoter of Nrg4 in mice inguinal white adipose tissue (iWAT) (Figure 1K). We further investigated the role of Ppary in exercise-mediated induction of adipose Nrg4 *in vivo*. Adeno-associated virus (AAV)-mediated knockdown of adipose Ppary impaired the role of exercise in promoting adipose Nrg4 expression (Figures 1L and 1M). These *in vivo* data further confirm that exercise induces adipose Nrg4 expression via Ppary. These results indicate that exercise induces upregulation of adipose Nrg4 in a Ppary-dependent manner.

Knockdown of adipose Nrg4 impairs exercise-mediated alleviation of MASLD in mice

To determine whether adipose Nrg4 is potentially involved in exercise-mediated protection against MASLD, we generated mice with adipose tissue-specific knockdown of Nrg4 via AAV delivery of short hairpin RNA (shRNA) to adipose tissues, including iWAT, eWAT, and BAT, as illustrated in Figures S1A and S1B. Then, mice were fed an HFD for 16 weeks to establish the MASLD model. From the ninth week of HFD feeding, mice were subjected to an established protocol of exercise (Trained) for 8 weeks (Figure 2A), with the mice kept in a sedentary lifestyle (Sed) as the non-exercising control.^{30,31} In shNC (non-specific control shRNA)-treated mice, exercise training significantly decreased body weight gain (Figures S1C and S1D), liver weight (Figure S1E), fat tissue weight (Figure S1F), and hepatic fat accumulation (Figures 2B–2D); improved glucose tolerance and insulin sensitivity (Figures 2E–2H); decreased serum alanine aminotransferase (ALT) and aspartate aminotransferase (AST) concentrations (Figures 2I and 2J); reduced the expression of lipogenic genes and inflammatory genes in the liver (Figure 2K); and decreased hepatic expression of the lipogenic protein stearoyl-CoA desaturase 1 (Scd1) (Figures 2L and S1G), in which the shNC/Trained group was compared to the shNC/Sed group. When comparing the shNrg4/Sed group to the shNC/Sed group, knockdown of adipose Nrg4 had little effect on body weight gain (Figures S1C and S1D). Knockdown of adipose Nrg4 (shNrg4/Sed group vs. shNC/Sed group) significantly exacerbated hepatic steatosis (Figures S1E and 2B–2D) and MASLD-associated disorders (Figures 2E–2L and S1G). Furthermore, when adipose Nrg4 was knocked down, the effect of exercise-mediated amelioration of MASLD phenotypes was blunted (shNrg4/Trained group vs. shNrg4/Sed group; Figures 2B–2L, S1E, and S1G). The expression levels of genes related to fatty acid β-oxidation (*Ppara* and *Cpt1a*) and fatty acid transportation (*Cd36*) were also examined in mouse livers. Knockdown of adipose Nrg4 had little effect on exercise-regulated expression of genes related to fatty acid

(H) HEK293T cells were transiently transfected with the WT or Mut reporter construct, along with the control vector or Ppary expression vector, and luciferase activities were then measured.

(I) 3T3-L1 adipocytes were treated with rosiglitazone (Rosi) for 12 h. The mRNA level of *Nrg4* was investigated.

(J) 3T3-L1 adipocytes were treated with Rosi (2 μM) for 12 h or left untreated. Then, Ppary enrichment on the *Nrg4* gene promoter was examined. Immunoglobulin G (IgG) served as a negative control.

(K) Ppary enrichment on the *Nrg4* gene promoter in the iWAT of mice.

(L and M) CD-fed 8-week-old WT male mice were administered adenoviruses harboring the indicated short hairpin RNAs (shRNAs) in the iWAT, eWAT, and BAT. After 1 week, mice were subjected to 8 weeks of exercise training or not. Ppary or *Nrg4* mRNA levels were examined in mouse adipose tissue.

Unpaired two-tailed t tests were performed in (B). One-way analysis of variance plus Tukey's post hoc tests were performed in (F), (G), and (I). Two-way analysis of variance plus Tukey's post hoc tests were performed in (H) and (J)–(M). All data show the mean ± SD. **p* < 0.05, ***p* < 0.01, ****p* < 0.001. ns, no significant difference. *n* = 6/group unless otherwise mentioned.

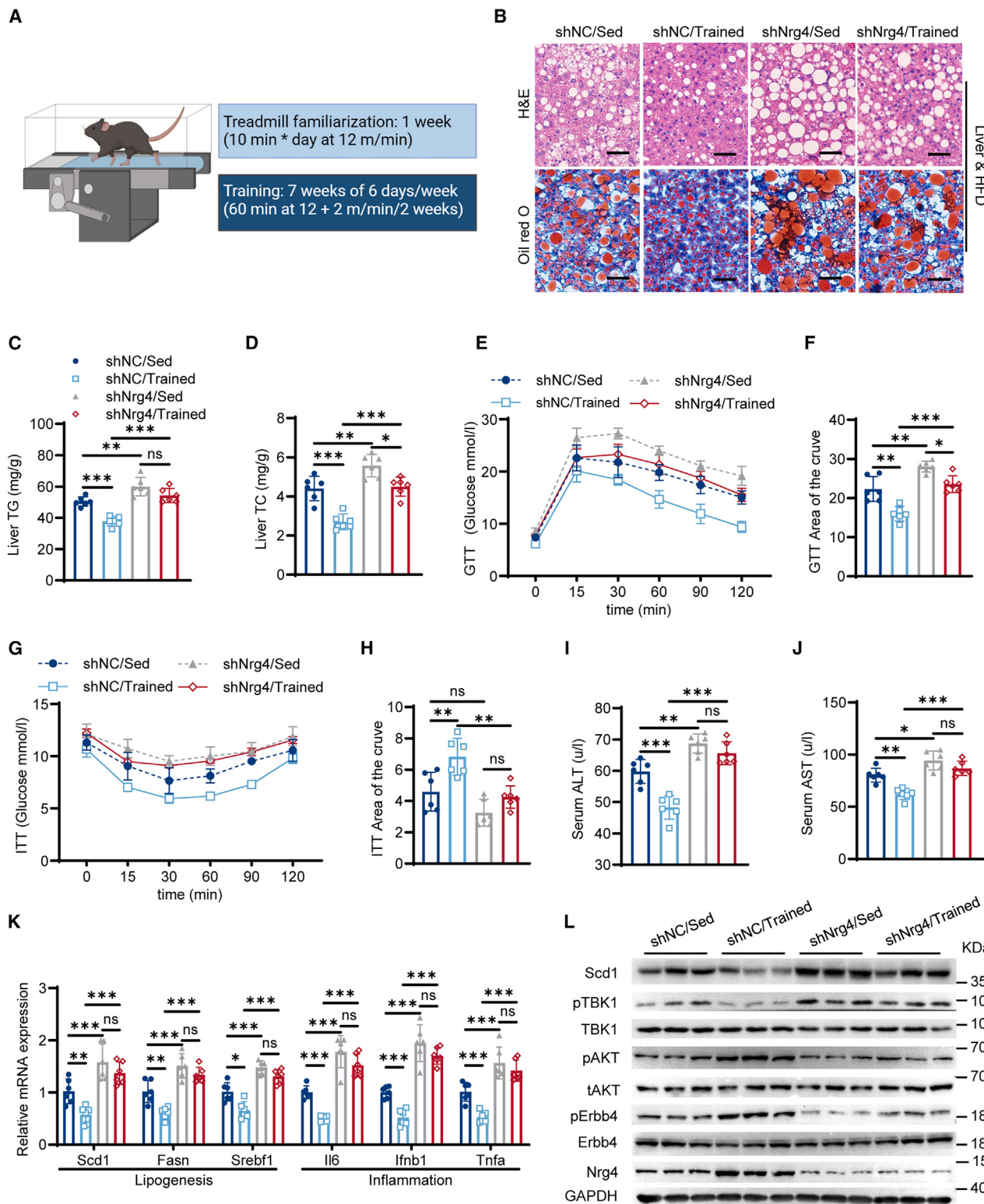


Figure 2. Knockdown of adipose Nrg4 impairs exercise-mediated alleviation of fatty liver in mice

(A) 6-week-old male mice were fed an high-fat diet (HFD) for 16 weeks with or without exercise in the last 8 weeks. WT male mice were administered AAVs harboring control shRNA (shNC) or the shRNA against murine Nrg4 (shNrg4) in the iWAT, eWAT, and BAT 1 week before exercise training. The exercise program is illustrated. The figure was created using BioRender.

(legend continued on next page)

β -oxidation (*Ppara* and *Cpt1a*) and fatty acid transportation (*Cd36*), as shown in Figure S1H. A metabolic cage experiment was also performed to show that exercise intervention promoted O₂ consumption, CO₂ emission, and heat production of the mice, and the effects mediated by exercise were not affected by knockdown of adipose Nrg4 (Figure S1I). These data are consistent with the results showing that knockdown of adipose Nrg4 had little effect on exercise-mediated reduction of body weight gain of the mice (Figures S1C and S1D). Additionally, in the HFD-fed mice, knockdown of adipose Nrg4 had little effect on exercise-mediated reduction of fat tissue weight (Figure S1F), promotion of catabolism-related gene expression (Figures S1J–S1L), and inhibition of inflammation gene expression in fat tissues (Figures S1J–S1L). These data suggest that adipose Nrg4 knockdown may blunt exercise-mediated alleviation of MASLD in mice without obvious effects on adipose metabolism.

Adipose Nrg4-regulated AKT and STING signaling are involved in exercise-mediated alleviation of MASLD in mice

AKT is one of the most critical and versatile protein kinases in higher eukaryotes. AKT have been identified as a signal factor regulated by Nrg4.^{19,21,32} Previous studies have shown that AKT in the liver is activated after exercise.^{33,34} Our western blot results indicated that the phosphorylated (p)-AKT (Ser473) level in mouse liver was also increased by exercise, but this effect was compromised by adipose knockdown of Nrg4 (Figures 2L and S1G). STING is an important pivot for cytosolic DNA sensation and interferon induction, promoting inflammation.³⁵ Previous studies have shown that inflammation-related factors are significantly downregulated by Nrg4 intervention.^{16,19,21} It has been reported that STING pathway-associated inflammatory factors, including *Tnf α* , *Il6*, *Il10*, and *Ifn β 1*, are significantly upregulated in 3T3-L1 adipocytes with Nrg4 knockdown.³⁶ Consistently, our results showed that STING-related inflammatory factors were significantly upregulated in the livers of mice with adipose tissue knockdown of Nrg4 (Figure 2K). The western blotting results showed that TRAF family member-associated Nf-kappa B activator binding kinase 1 (TBK1), a downstream signaling factor of STING, was significantly activated in the livers of mice with adipose knockdown of Nrg4 (Figures 2L and S1G). Importantly, exercise-mediated inhibition of hepatic inflammatory factor expression and TBK1 activation was significantly attenuated by knockdown of adipose Nrg4 (Figures 2K, 2L, and S1G). Thus, adipose Nrg4 contributes to the alleviation of MASLD by exercise, in which AKT and STING signaling are involved.

Hepatic Nrg4/ErbB4 signaling facilitates exercise-mediated alleviation of MASLD

The Erbb4 receptor tyrosine kinase is known to be the receptor of Nrg4.^{16,21} We hypothesize that Nrg4 inhibits hepatosteatosis and hepatic inflammation through the Erbb4 receptor tyrosine kinase. To verify this hypothesis *in vitro*, we evaluated the role of Nrg4 in hepatic steatosis and inflammation by using mouse primary hepatocytes that were treated with free fatty acids (FFAs), as shown in Figures S2A–S2D. Nrg4 treatment protected FFA-induced hepatocyte steatosis and inflammation, as evidenced by decreased lipid accumulation (Figures 3A and S2E), downregulated expression of lipogenic genes and inflammatory genes (Figure 3B), increased activation of AKT, and decreased activation of TBK1 (Figures 3C and S2F) when compared to the vehicle control group. The Erbb4 receptor tyrosine kinase was activated upon Nrg4 treatment (Figures 3C and S2F). After knockdown of the Erbb4 receptor, Nrg4-mediated inhibition of hepatosteatosis and TBK1 activation as well as activation of AKT were blunted (Figures 3D–3F and S2G).

Furthermore, we queried whether hepatocyte ErbB4 is involved in exercise-mediated alleviation of MASLD in mice. Thus, we generated hepatic-specific Erbb4 knockout (Erbb4^{LKO}) mice and the control Erbb4^{fl/fl} mice (WT control). The specific deletion of Erbb4 in hepatocytes was validated (Figures S2H and S2I). The 6-week-old Erbb4^{LKO} and control WT mice were fed an HFD for 16 weeks and were subjected to treadmill training or not in the last 8 weeks. As expected, The WT/Trained mice had less lipid accumulation in the liver (Figures 3G and 3H), lower serum ALT/AST levels (Figures 3I and 3J), lower expression levels of lipogenic genes and inflammatory genes (Figure 3K), and reduced TBK1 activation and increased AKT and Erbb4 activation (Figures 3L and S2J) as compared to WT/Sed mice. However, Erbb4^{LKO} led to more severe fatty liver phenotypes and blunted the role of exercise-mediated alleviation of MASLD in mice (Figures 3G–3L and S2J). Therefore, these data indicate that Nrg4/ErbB4 signaling plays an important role in the alleviation of MASLD in mice brought about by exercise.

Inhibition of STING-induced inflammation contributes to Nrg4-mediated amelioration of hepatocyte steatosis

TBK1 is an important downstream effector of the cGAS-STING pro-inflammatory pathway.³⁷ Our data demonstrated that cGAS-STING pathway-induced inflammatory factor expression and TBK1 activation were significantly affected in the livers of mice by exercise and adipose knockdown of Nrg4 (Figures 2K and 2L). Therefore, we examined the role of the cGAS-STING

(B–L) Mice were treated as described in (A) before being sacrificed for analysis ($n = 6$ mice/group).

(B) Representative images of hematoxylin and eosin (H&E) staining and oil red O staining of liver sections. Scale bars, 50 μ m.

(C and D) Triglyceride (TG) and total cholesterol (TC) levels in mouse livers, respectively.

(E) A glucose tolerance test (GTT) was performed in mice under 14 weeks of HFD feeding.

(F) Analysis of the GTT data in (E) with subtraction of the basal glucose to generate an area of the curve (AOC).

(G) An insulin tolerance test (ITT) was performed in mice fed an HFD for 15 weeks.

(H) Analysis of the ITT data in (G) with AOC.

(I and J) Serum alanine aminotransferase (ALT) and serum aspartate aminotransferase (AST) levels in mice, respectively.

(K) The mRNA levels of the indicated genes in mouse livers.

(L) Western blot of the mouse liver lysates ($n = 3$ mice/group).

Two-way analysis of variance plus Tukey's post hoc tests were performed in (C), (D), (F), and (H)–(K). All data show the mean \pm SD. * $p < 0.05$, ** $p < 0.01$, *** $p < 0.001$.

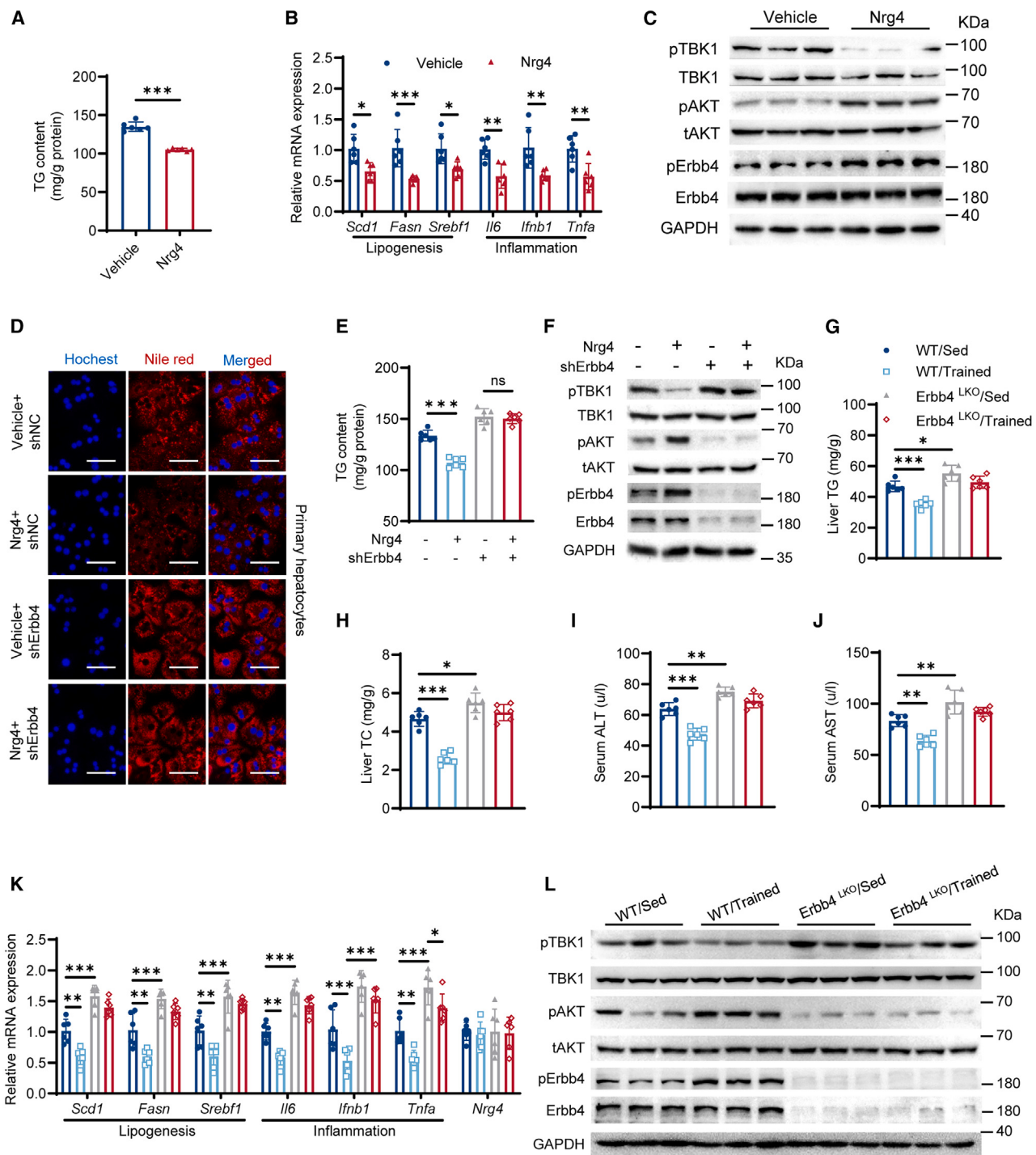


Figure 3. Hepatic Nrg4/Erbb4 signaling facilitates exercise-mediated alleviation of MASLD

(A–C) Mice primary hepatocytes were treated with a mixture of 0.6 mM FFAs (oleate and palmitate) at a final ratio of 2:1 for 36 h with or without recombinant Nrg protein (100 ng/mL) treatment in the last 24 h. Then, cells were harvested and analyzed.

(A) TG levels in primary hepatocytes.

(B) The mRNA levels of the indicated genes.

(C) Western blot of the cell lysates.

(D–F) WT primary hepatocytes were infected with adenoviruses harboring the indicated shRNAs. After 24 h, cells were treated with FFAs and Nrg4 as described in (A)–(C). Then, cells were harvested and analyzed.

(legend continued on next page)

signaling pathway in Nrg4-mediated amelioration of hepatosteatosis. When we used a STING agonist in FFA-treated primary hepatocytes, it was found that the effects of Nrg4 on the alleviation of hepatic steatosis were abolished (Figures 4A and 4B). Consistently, Nrg4-mediated inhibition of TBK1 phosphorylation and lipogenic gene and inflammation gene expression were blunted by treatment with the STING agonist (Figures 4C–4E). Then, we silenced STING expression in primary hepatocytes via shRNA-mediated knockdown of STING. It was found that the alleviation of hepatocyte steatosis and the inhibition of lipogenic gene and inflammation gene expression, brought about by Nrg4 treatment, were impaired by the knockdown of STING (Figures 4F–4J). We further validated, in HFD-fed mice, that both overexpression of adipose Nrg4 and knockdown of hepatic STING led to inhibition of TBK1 phosphorylation and decreased expression of lipogenic genes and inflammation genes in mouse livers (Figures 4K–4M). However, overexpression of adipose Nrg4 did not further suppress TBK1 phosphorylation or the expression of lipogenic genes or inflammation genes in mouse livers when hepatic STING was knocked down (Figures 4K–4M). These results demonstrate that the inhibition of STING-induced inflammation plays an important role in Nrg4-mediated amelioration of hepatocyte steatosis.

Nrg4/Erbb4 signaling inhibits the cGAS-STING pathway by activating AKT

cGAS has been characterized as a primary cytosolic DNA sensor that converts ATP and guanosine triphosphate (GTP) into the dinucleotide cyclic GMP-AMP (cGAMP).^{35,38} cGAMP is a second messenger that binds to STING, which, in turn, induces the recruitment of TBK1 to form a complex with STING.^{35,38} Whether Nrg4 regulates STING-induced inflammation in a cGAS-dependent manner was investigated. We examined the levels of cGAMP in the livers of HFD-fed mice after adipose tissue-specific knockdown of Nrg4 as well as exercise intervention. The livers of shNC/Trained mice had lower cGAMP levels than those of shNC/Sed mice (Figure 5A). Knockdown of adipose Nrg4 led to more accumulation of hepatic cGAMP and also compromised the role of exercise in reducing the accumulation of hepatic cGAMP (Figure 5A). In addition, Nrg4 treatment significantly decreased cGAMP levels in FFA-treated primary hepatocytes, and this effect was abolished by knockdown of Erbb4 (Figure 5B). Furthermore, when the cGAS enzyme activity was inhibited, Nrg4 did not further inhibit the activation of TBK1 or the expression of lipogenic genes and inflammation genes in FFA-treated primary hepatocytes (Figures 5C–5E). Then, it was found that both overexpression of adipose Nrg4

and knockdown of hepatic cGAS led to inhibition of TBK1 phosphorylation and decreased expression of lipogenic genes and inflammation genes in mouse livers (Figures 5F–5H). However, overexpression of adipose Nrg4 did not further suppress TBK1 phosphorylation or the expression of lipogenic genes or inflammation genes in mouse livers when hepatic cGAS was knocked down (Figures 5F–5H).

Previous studies have shown that Erbb4/AKT signaling is involved in the beneficial effects of Nrg4.^{19,21,32} Thus, we investigated the potential role of AKT in Nrg4/Erbb4 pathway-mediated inhibition of the cGAS-STING signaling pathway. As indicated, when AKT activity was inhibited in FFA-treated primary hepatocytes, Nrg4-mediated inhibition of TBK1 activation (Figures 5I and 5J) and decrease of cGAMP levels (Figure 5K) were impaired. These results demonstrate that Nrg4/Erbb4/AKT signaling suppresses the cGAS-STING pathway, which helps to alleviate inflammation and steatosis in hepatocytes.

Nrg4/Erbb4/AKT signaling leads to phosphorylation of cGAS to inhibit its enzyme activity and STING-induced inflammation

Next, the molecular mechanism of Nrg4/Erbb4 signaling-mediated inhibition of the cGAS-STING inflammation pathway was investigated. At the endogenous level, it was found that Erbb4 formed a complex with AKT and cGAS, and this interaction was enhanced by Nrg4 treatment, which was blunted upon inhibition of Erbb4 activity (Figures 6A, 6B, and S3A). The interaction of cGAS with AKT in response to Nrg4-Erbb4 signaling axis activation was detected directly in hepatocytes. Nrg4 treatment enhanced the interaction of AKT with cGAS, but this interaction was impaired when Erbb4 activity was inhibited (Figures S3B–S3D). Furthermore, phosphorylation of AKT was also detected in this context. Nrg4 treatment promoted AKT phosphorylation in both the input samples and the immunoprecipitation (IP) samples, which were blunted upon inhibition of Erbb4 activity (Figures S3B–S3D). Our data showed that AKT enzyme activity was important for Nrg4/Erbb4 signaling-mediated inhibition of cGAS enzyme activity (Figures 5I–5K). Previous studies have shown that the cGAS sequence around serine 305 (S305) includes a known target motif for AKT kinase (R/KXR/KXX*S/T; X, any amino acid) that is highly conserved across multiple species.³⁹ In mouse cGAS, the homologous residue is serine 291 (S291). Because of the proximity of S305 or S291 to the catalytic site of human or mouse cGAS, respectively, we hypothesize that AKT mediates cGAS phosphorylation at this site to control cGAS enzymatic activity. To validate AKT-mediated phosphorylation of

(D) Nile red and Hoechst staining of the cells. Scale bars, 50 μm.

(E) TG levels in primary hepatocytes.

(F) Primary hepatocyte lysates were analyzed by western blotting with the indicated antibodies. A representative blot is shown.

(G–L) 6-week-old Erbb4^{flox/flox} (WT) and Erbb4^{LKO} male mice were fed an HFD for 16 weeks with or without exercise in the last 8 weeks. The exercise intervention program is illustrated Figure 2A.

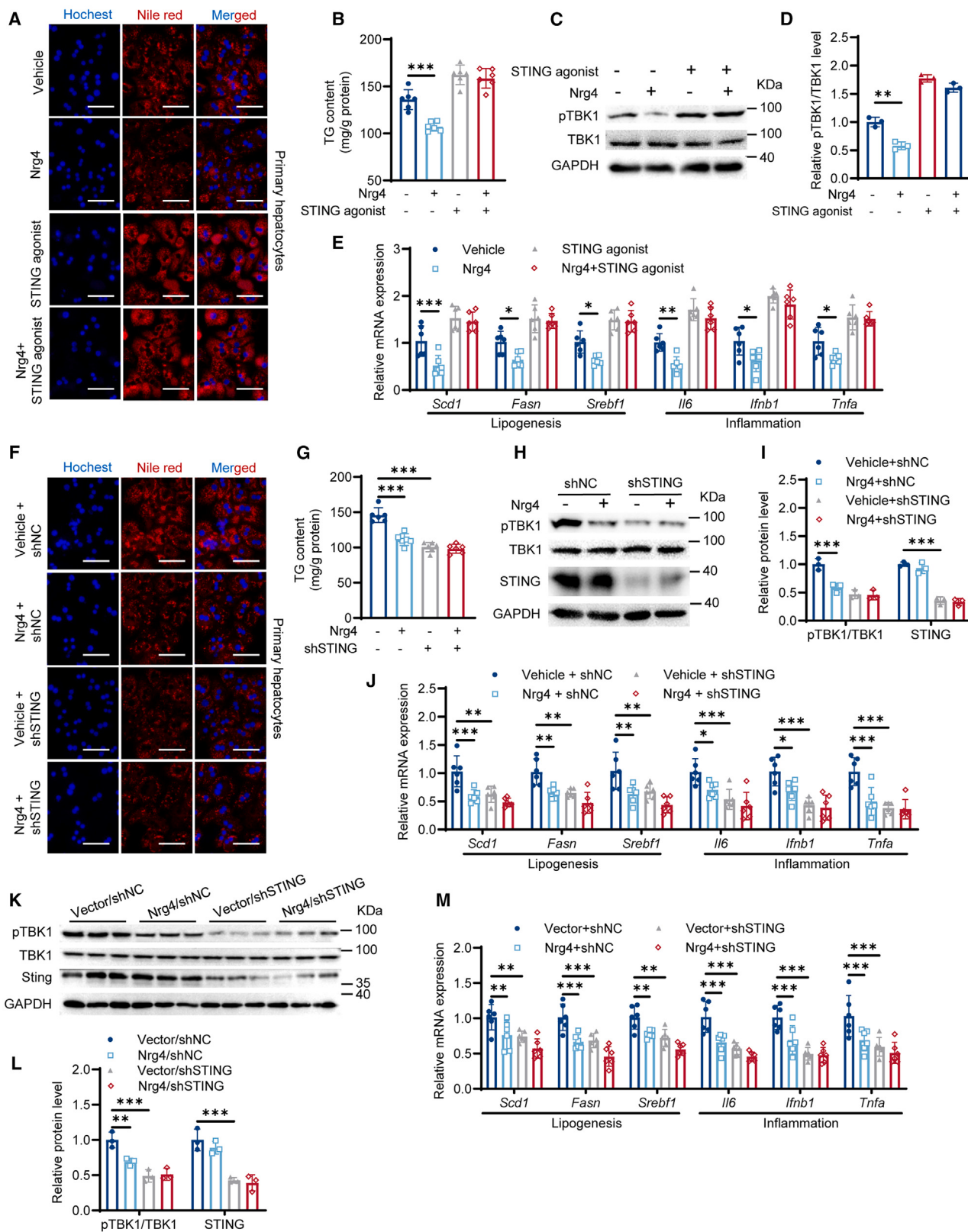
(G and H) TG and TC levels in mouse livers, respectively.

(I and J) Serum ALT and serum AST levels in mice, respectively.

(K) The mRNA levels of the indicated genes in mouse livers.

(L) Western blot of the indicated proteins in mouse livers.

Unpaired two-tailed t tests were performed in (A) and (B). Two-way analysis of variance plus Tukey's post hoc tests were performed in (E) and (G)–(K). $n = 3$ independent biological replicates/group for western blot results. $n = 6$ independent biological replicates/group for other experiments. All data show the mean ± SD. * $p < 0.05$, ** $p < 0.01$, *** $p < 0.001$.



(legend on next page)

murine cGAS on S291, WT mouse FLAG-cGAS-WT or mutant mouse FLAG-cGAS-S291A was overexpressed in mouse primary hepatocytes, followed by treatment with Nrg4 recombinant protein. Cell lysates were then subjected to IP with an anti-FLAG antibody to obtain the immunoprecipitated FLAG-cGAS-WT or FLAG-cGAS-S291A. The immunoprecipitated samples were immunoblotted with an AKT phosphosubstrate antibody that specifically recognizes the phosphorylated consensus motif K/RXK/RXXpS/pT. Mouse FLAG-cGAS-WT proteins were detected by the AKT phosphosubstrate antibody, and this immunoblot signal was apparently enhanced upon treatment with Nrg4 recombinant protein (Figures 6C, 6D, and S3E). However, the FLAG-cGAS-S291A protein was not recognized by the anti-AKT phosphosubstrate antibody (Figures 6C, 6D, and S3E). To further validate the role of cGAS S291 phosphorylation in the beneficial effects mediated by Nrg4, primary hepatocytes with knockdown of endogenous cGAS were subjected to ectopic expression of either the wild-type cGAS (cGAS-WT) or the mutant cGAS with mutation of serine (S) to alanine (A) at the amino acid position of 291 (cGAS-S291A) (Figures S3F and S3G). In primary hepatocytes expressing cGAS-WT, Nrg4 efficiently inhibited TBK1 activation (Figures 6E and 6F), decreased cGAMP levels (Figure 6G), reduced the expression of inflammation genes (*Tnfa*, *Ifnb1*, and *Il6*) and lipogenic genes (*Scd1*, *Fasn*, and *Srebf1*) (Figure 6H), and alleviated hepatosteatosis (Figure 6I). However, these effects of Nrg4 were abolished in primary hepatocytes with ectopic expression of FLAG-cGAS-S291A (Figures 6E–6I). Collectively, these results demonstrate that Nrg4/ErbB4/AKT signaling leads to the phosphorylation of cGAS on S291, which inhibits cGAS enzyme activity to impair STING-induced inflammation and steatosis in hepatocytes.

Adipose overexpression of Nrg4 and exercise synergistically alleviate MASLD in mice

We next carried out gain-of-function experiments by delivering AAVs to interscapular BAT, iWAT, and eWAT for overexpression

of adipose Nrg4 (Figure 7A). Then, mice were fed an HFD for 16 weeks and subjected to treadmill training or not in the last 8 weeks (Figure S4A). Exercise training, but not Nrg4 overexpression, decreased the body weight gain of the mice (Figures S4B–S4D). In addition, compared to the control group of mice (Vector/Sed), exercise alone (Vector/Trained) or Nrg4 overexpression alone (Nrg4/Sed) decreased the liver weight (Figure S4E) and lipid accumulation in the liver (Figures 7B–7D), improved glucose tolerance and insulin sensitivity (Figures 7E–7H), led to lower serum levels of ALT and AST (Figures 7I and 7J), decreased the expression of lipogenesis and inflammation genes (Figure 7K), inhibited TBK1 phosphorylation and Scd1 protein expression (Figures 7L and S4F), and promoted Erbb4 and AKT activation (Figures 7L and S4F). It is worth mentioning that the combination of exercise and Nrg4 (Nrg4/Trained) yielded better effects on inhibiting fatty liver and the associated phenotypes (Figures 7B–7L, S4E, and S4F). These results demonstrated that adipose Nrg4 and exercise can cooperate to alleviate MASLD in mice, in which Nrg4/ErbB4/AKT signaling-mediated inhibition of STING-induced hepatic inflammation is involved.

DISCUSSION

Elucidating mechanisms that underlie the profound benefits of exercise for human health has been a major research challenge, with most studies focusing on adaptation of skeletal muscle to exercise. Our findings indicate that Nrg4 is an adipokine that is induced upon exercise training in mice and provide insight into exercise-mediated adipose-liver tissue communication to counteract hepatic inflammation and steatosis. We show that Nrg4 is an exercise-induced adipokine via Ppary-triggered transactivation and facilitates exercise-mediated alleviation of MASLD via Nrg4/ErbB4/AKT axis-mediated inhibition of cGAS-STING inflammatory signaling in hepatocytes. In the current study, we establish a paradigm in which adipose tissue plays an important

Figure 4. Inhibition of STING-induced inflammation contributes to Nrg4-mediated amelioration of hepatocyte steatosis

(A–E) WT primary hepatocytes were treated with a mixture of 0.6 mM FFAs (oleate and palmitate) at a final ratio of 2:1 for 36 h with or without a STING agonist (diABZI STING agonist, 1 μM) in the last 26 h and with or without recombinant Nrg4 protein (100 ng/mL) in the last 24 h. Then, cells were harvested and analyzed. (A) Nile red and Hoechst staining of the cells. Scale bars, 50 μm.

(B) TG levels in primary hepatocytes.

(C) Primary hepatocyte lysates were analyzed by western blotting with the indicated antibodies.

(D) Quantification of the western blot results in (C).

(E) The mRNA levels of the indicated genes.

(F–J) WT primary hepatocytes were infected with adenoviruses harboring the indicated shRNAs. After 24 h, cells were treated with a mixture of 0.6 mM FFAs (oleate and palmitate) at a final ratio of 2:1 for 36 h with or without recombinant Nrg4 protein (100 ng/mL) in the last 24 h. Then, cells were harvested and analyzed.

(F) Nile red and Hoechst staining of the cells. Scale bars, 50 μm.

(G) TG levels in primary hepatocytes.

(H) Primary hepatocyte lysates were analyzed by western blotting with the indicated antibodies.

(I) Quantification of the western blot results in (H).

(J) The mRNA levels of the indicated genes.

(K–M) 6-week-old WT male mice were fed an HFD for a total of 6 weeks. WT male mice were administered adenoviruses harboring the indicated shRNAs in the iWAT, eWAT, and BAT at the end of 2 weeks and 4 weeks of HFD feeding. These mice were administered AAVs harboring a control vector or the vector expressing murine Nrg4 in the iWAT, eWAT, and BAT at the end of 3 weeks of HFD feeding. Mice were sacrificed for analysis after 6 weeks of HFD feeding.

(K) The mouse liver lysates were analyzed by western blotting.

(L) Quantification of the western blot results in (K).

(M) The mRNA levels of the indicated genes were determined.

Two-way analysis of variance plus Tukey's post hoc tests were performed in (B), (D), (E), (G), (I), (J), (L), and (M). All data show the mean ± SD. **p* < 0.05, ***p* < 0.01, ****p* < 0.001. *n* = 3 independent biological replicates/group for western blot results. *n* = 6 independent biological replicates/group for other experiments.

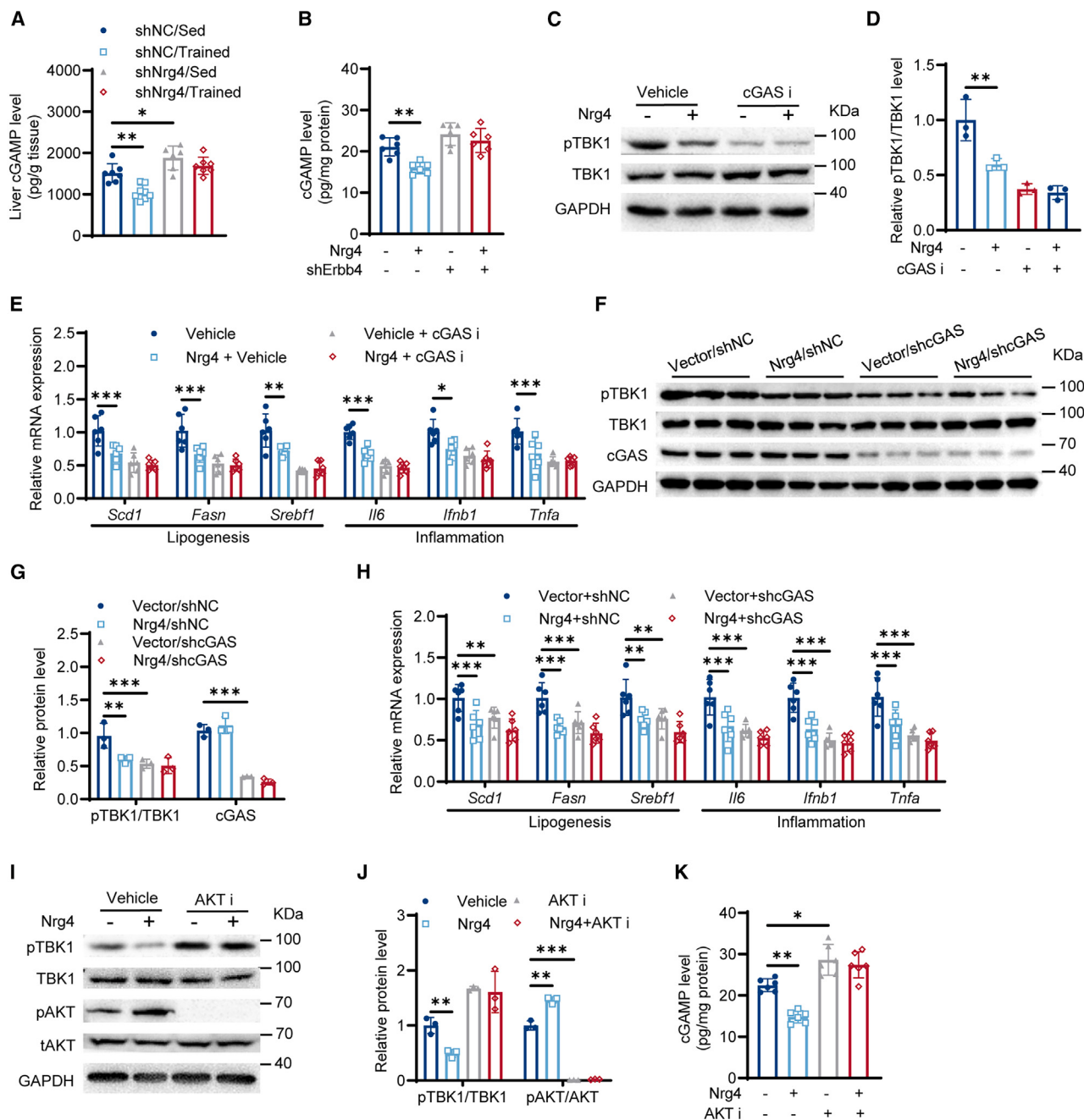


Figure 5. Nrg4/ErbB4 signaling inhibits the cGAS-STING pathway by activating AKT

- (A) Mice were treated as described in Figure 2A. Shown are the cGAMP levels in mouse liver.
- (B) WT primary hepatocytes were treated as described in Figure 3D. The cGAMP levels in primary hepatocytes were determined.
- (C-E) WT primary hepatocytes were treated with a mixture of 0.6 mM FFAs (oleate and palmitate) at a final ratio of 2:1 for 36 h with or without a cGAS inhibitor (RU.521, 10 μ M) in the last 26 h and with or without recombinant Nrg4 protein (100 ng/mL) in the last 24 h. Then, cells were harvested and analyzed.
- (C) Primary hepatocyte lysates were analyzed by western blotting.
- (D) Quantification of the western blot results in (C).
- (E) The mRNA levels of the indicated genes.
- (F-H) 6-week-old WT male mice were fed an HFD for a total of 6 weeks. Mice were administered adenoviruses harboring the indicated shRNAs in the iWAT, eWAT, and BAT at the end of 2 weeks and 4 weeks of HFD feeding. These mice were administered AAVs harboring a control vector or the vector expressing murine Nrg4 in the iWAT, eWAT, and BAT at the end of 3 weeks of HFD feeding. Mice were sacrificed for analysis after 6 weeks of HFD feeding.
- (F) The mouse liver lysates were analyzed by western blotting.
- (G) Quantification of the western blot results in (F).

(legend continued on next page)

role in exercise training adaptation, which helps to ameliorate MASLD.

Regular exercise can reduce the risk of developing MASLD.^{40–43} Previous studies have shown that some exercise-induced secreted factors, such as growth differentiation factor 15 (GDF15), adiponectin, irisin, and so on, have potential roles in improving liver function and alleviating MASLD. Elevation of hepatic GDF15 expression promotes fatty acid oxidation to reduce fat accumulation in the liver and inhibit the development of MASLD in obese mice.^{44,45} Adiponectin improves insulin sensitivity and inhibits hepatic inflammation in HFD-fed mice.⁴⁶ Irisin improves lipid metabolism and alleviates inflammation in palmitic acid-treated hepatocytes, which may play roles in the amelioration of MASLD.⁴⁷ However, more studies are needed to confirm the contribution of these exerkines to exercise-induced alleviation of MASLD. Here, we show that Nrg4, as an exerkine, mediates adipose-liver tissue crosstalk to counteract MASLD. Exercise promotes expression of adipose Nrg4, which directly binds to Erbb4 on the hepatocyte cell surface, which protects against diet-induced hepatic steatosis by attenuating hepatic inflammation and lipogenesis. Knockdown of adipose Nrg4 impairs exercise-induced amelioration of MASLD in mice, which suggests an important role of adipose Nrg4 in the ameliorative effects of exercise on MASLD. In pathological conditions, BAT-derived Nrg4 restoration alleviates vascular inflammation in atherosclerosis in male mice²¹; exogenous Nrg4 treatment attenuates renal function injury, tubulointerstitial fibrosis, and inflammation and suppresses the expression levels of advanced glycosylation end products in diabetic nephropathy of rats⁴⁸; and Nrg4 intervention attenuates diabetic cardiomyopathy by promoting autophagy in type 1 diabetic mice.⁴⁹ Therefore, further studies are needed to investigate the potential role of adipose Nrg4 in exercise-mediated amelioration of these diseases.

cGAMP is a second messenger molecule and potent agonist of STING.^{35,50} Within this pathway, cGAS senses misplaced genomic, mitochondrial, and microbial double-stranded DNA to synthesize cGAMP, which mobilizes STING to unleash innate immune responses, constituting a ubiquitous and effective surveillance system against tissue damage and pathogen invasion.^{50,51} Recently, the interaction between cGAS-STING signaling and lipid and glucose metabolism was demonstrated,⁵² which may be involved in some metabolic diseases, such as obesity, insulin resistance, and fatty liver diseases. The perturbation of fatty acid metabolism can activate the cGAS-STING machinery,⁵³ and the imbalance between cholesterol synthesis and import also affects the STING-mediated interferon response.⁵⁴ A study found that STING knockdown significantly reduces the FFA-induced hepatocyte inflammatory response and lipid accumulation.⁵⁵ In addition, STING overex-

pression in primary hepatocytes exacerbates abnormal lipid accumulation induced by FFAs, accompanied by increased expression of genes associated with inflammation and lipogenesis.⁵⁶ Furthermore, a study has shown that 8 weeks of aerobic exercise reduces inflammation in the heart of HFD-induced obese mice by effectively suppressing the STING signaling pathway.⁵⁷ The STING signal is significantly activated in MASLD,^{50,58–60} but whether exercise affects the hepatic STING signaling pathway in MASLD is unclear. Our study found that exercise-induced adipose Nrg4 promotes cGAS phosphorylation, thereby inhibiting cGAS-STING pathway-mediated inflammation and steatosis in hepatocytes. Our work provides mechanistic insight into exercise-mediated alleviation of MASLD.

cGAS converts ATP and GTP into the dinucleotide cGAMP in a process that involves a conformational change at the cGAS active site. cGAMP is a second messenger that binds to STING, which activates TBK1 through a phosphorylation-dependent mechanism.^{37,59,61} Current studies of cGAS have focused on its DNA-sensing mechanism and activation in immune and inflammatory programs.^{62,63} Notably, the enzyme activity of cGAS can be inhibited by its phosphorylation in HeLa cells.⁶⁴ In our search in the literature for the kinases that phosphorylate cGAS, we noticed that the kinetics of cGAS modification strongly correlated with AKT,³⁹ a well-known target of Nrg4/Erbb4.^{19,21,32} High-quality higher-energy collisional dissociation spectra have identified several potential phosphorylated serine and phosphorylated threonine residues in cGAS, in which Ser305 (human) or Ser291 (mouse) is within the catalytic domain of cGAS.^{39,64} Our data reveal that AKT leads to Ser291 phosphorylation in mouse cGAS, which blunts cGAS enzyme activity to produce less cGAMP in hepatocytes. Consistently, Nrg4/Erbb4 promotes AKT-mediated phosphorylation of cGAS (Ser291), thereby inhibiting the cGAS-STING pathway to attenuate hepatic inflammation and steatosis (Figures 5 and 6). As far as we know, no studies have reported the role of Nrg4-Erbb4 signaling in the regulation of the cGAS-STING inflammatory pathway. Our current work provides mechanistic insight into the protective role of adipose Nrg4 in MASLD, in which hepatic Erbb4-cGAS-STING signaling is involved. Our study helps to better understand the functional role and the underlying mechanism of Nrg4 in promoting metabolic health, which paves the way for Nrg4-based therapeutic strategies against metabolic diseases such as MASLD.

MASLD is commonly associated with inflammation in liver tissue,^{65–67} while exercise training is recognized for decreasing hepatic triglycerides and inducing anti-inflammatory effects.^{47,68,69} Our current findings demonstrate that treadmill exercise training induced the expression of adipose Nrg4 to mitigate MASLD in HFD-fed mice. Although some studies have shown that Nrg4

(H) The mRNA levels of the indicated genes.

(I–K) WT primary hepatocytes were treated with a mixture of 0.6 mM FFAs (oleate and palmitate) at a final ratio of 2:1 for 36 h with or without an AKT inhibitor (10 μM) in the last 26 h and with or without recombinant Nrg4 protein (100 ng/mL) in the last 24 h.

(I) Cell lysates were analyzed by western blotting.

(J) Quantification of the western blot results in (I).

(K) The cGAMP level in primary hepatocytes.

Two-way analysis of variance plus Tukey's post hoc tests were performed in (A), (B), (D), (E), (G), (H), (J), and (K). All data show the mean ± SD. **p* < 0.05. ***p* < 0.01, ****p* < 0.001. *n* = 3 independent biological replicates/group for western blot results. *n* = 6 independent biological replicates/group for other experiments.

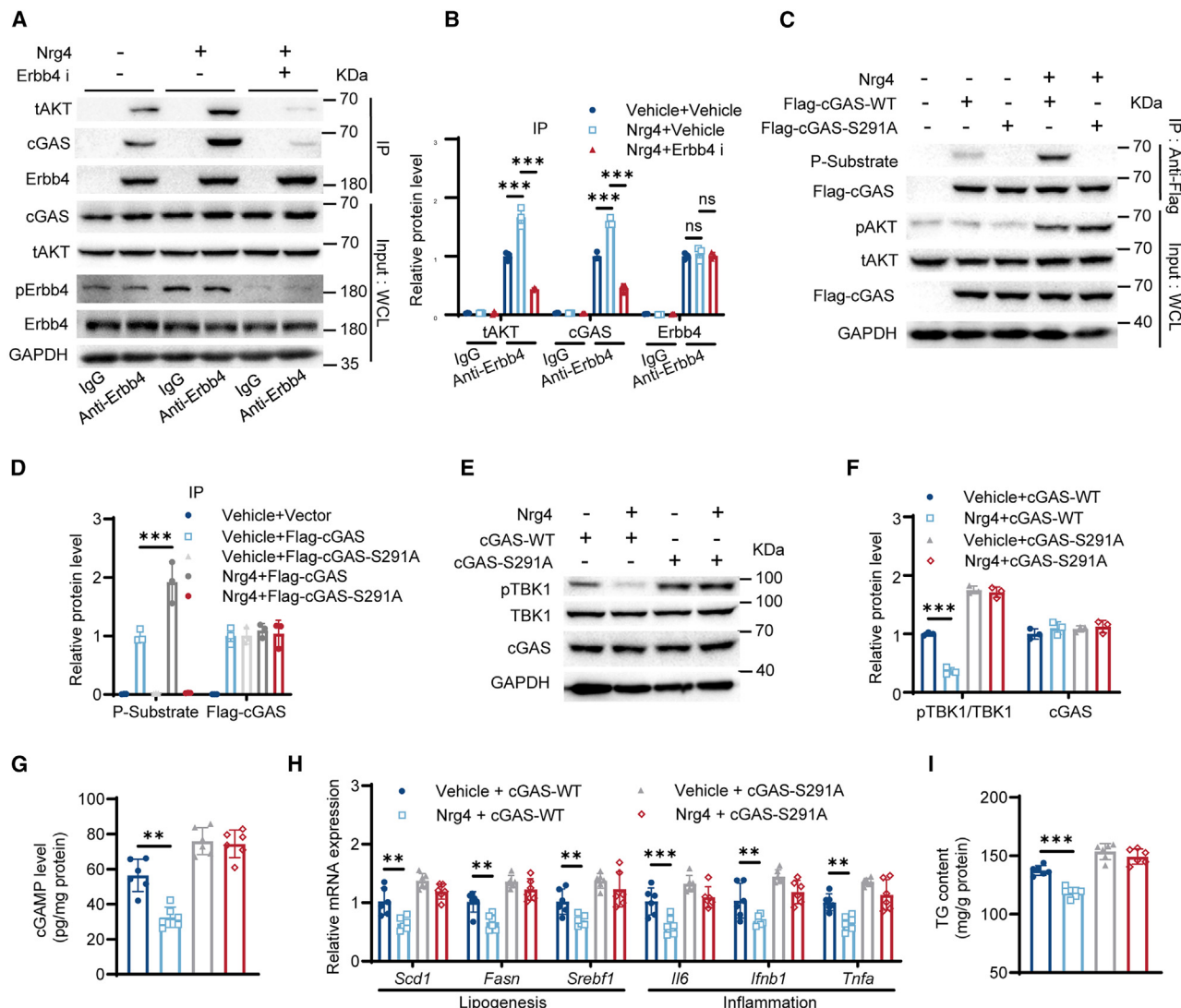


Figure 6. Nrg4/Erbb4/AKT signaling leads to phosphorylation of cGAS to inhibit its enzyme activity and STING-induced inflammation

(A) WT primary hepatocytes were treated with a mixture of 0.6 mM FFAs (oleate and palmitate) at a final ratio of 2:1 for 24 h with or without an Erbb4 inhibitor (afatinib, 1 μ M) in the last 2 h and with or without recombinant Nrg4 protein (100 ng/mL) in the last 0.5 h. Cell lysates were then immunoprecipitated with the antibody against Erbb4, followed by western blotting. WCL, whole cell lysate.

(B) Quantification of the immunoprecipitation (IP) results in (A).

(C) Primary hepatocytes were infected with an adenovirus (AD) harboring FLAG-cGAS-WT or FLAG-cGAS-S291A. After 24 h, cells were treated with recombinant Nrg4 protein (100 ng/mL) for 0.5 h. IP was performed using an anti-FLAG antibody followed by western blotting with antibodies as indicated.

(D) Quantification of the IP results in (C).

(E–I) Primary hepatocytes with knockdown of endogenous cGAS were infected with AD harboring FLAG-cGAS-WT or FLAG-cGAS-S291A. After 24 h, cells were treated with FFAs as described in (A) for 36 h with or without recombinant Nrg4 protein (100 ng/mL) in the last 24 h.

(E) Primary hepatocyte lysates were analyzed by western blotting with the indicated antibodies.

(F) Quantification of the western blot results in (E).

(G) The cGAMP levels in primary hepatocytes.

(H) The mRNA levels of the indicated genes.

(I) TG levels in primary hepatocytes.

Two-way analysis of variance plus Tukey's post hoc tests were performed in (B), (D), and (F)–(I). All data show the mean \pm SD. * p < 0.05, ** p < 0.01, *** p < 0.001. n = 3 independent biological replicates/group for western blot results. n = 6 independent biological replicates/group for other experiments.

levels can be upregulated by exercise,¹⁸ the underlying mechanism is not clear. There are multiple potential mechanism underlying it. For example, exercise may promote the transcription,

mRNA stability, or translation of the *Nrg4* gene or may enhance the stability of the Nrg4 protein, which awaits further dissection. A previous study hinted that PPAR γ can regulate Nrg4

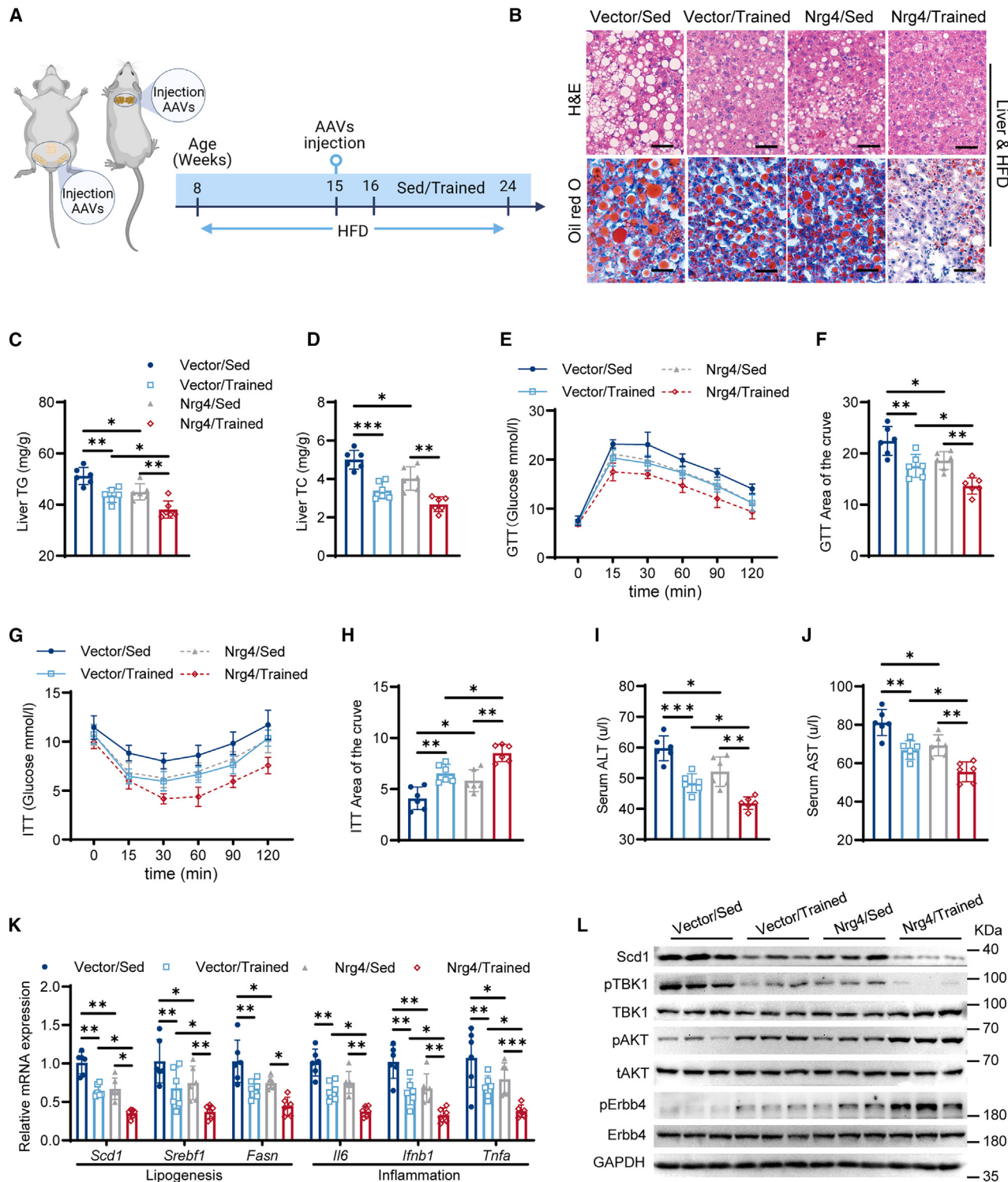


Figure 7. Overexpression of adipose Nrg4 and exercise synergistically alleviate MASLD in mice

(A) 6-week-old male mice were fed an HFD for 16 weeks with or without exercise in the last 8 weeks. Mice were administered AAVs harboring a control vector or the vector expressing murine Nrg4 in the iWAT, eWAT, and BAT 1 week before exercise training. After this intervention, mice were sacrificed for analysis. The figure was created using BioRender.

(B) Representative images of H&E staining and oil red O staining. Scale bars, 50 μ m.
(C and D) TG and cholesterol (TC) levels in mouse livers ($n = 6$ mice/group).

(legend continued on next page)

expression,⁷⁰ but whether PPAR γ can definitely regulate Nrg4 expression and the exact molecular mechanism underlying this regulation are still not known. Our current work provides strong evidence that exercise can induce adipose Nrg4 expression by promoting transcription of the *Nrg4* gene in a PPAR γ -dependent manner (Figures 1L and 1M). Our *in vivo* and *in vitro* data also indicate that PPAR γ can directly bind to the promoter of the *Nrg4* gene to transactivate its expression, which plays an important role in mediating the induction of adipose Nrg4 by exercise (Figures 1C–1M). Together, these results unravel a previous unknown adipose PPAR γ /Nrg4 axis in response to exercise intervention, which contributes to the protective effects of exercise against MASLD.

Randomized controlled trials in 551 adults with MASLD showed that exercise training subjects were more likely to achieve $\geq 30\%$ relative reduction in MRI-measured liver fat than those under the control condition.⁷¹ However, many MASLD patients are challenged by weight issues such as being overweight or obese, which not only increases the difficulty of starting and maintaining exercise but may also affect their adherence to effective exercise programs.^{72,73} Therefore, developing a strategy aimed at enhancing the benefits of exercise or reducing the barriers to its execution is particularly important.⁷⁴ In our study, we found that exercise alone or adipose Nrg4 overexpression alone can inhibit lipogenesis and inflammation in the mouse liver. The combination of exercise and Nrg4 led to a significant further amelioration of MASLD phenotypes. This may provide measures for enhancing the effect of exercise on the prevention and control of MASLD.

In our work, the mechanism underlying the induction of adipose Nrg4 by exercise is identified. Our results also illustrate an exercise-mediated adipose tissue/liver axis in which adipose Nrg4 regulates hepatic Erbb4-cGAS-STING signaling to alleviate hepatic steatosis, providing mechanistic insight into the ameliorative effect of exercise on MASLD. Furthermore, the additive effects of adipose Nrg4 overexpression and exercise on alleviating hepatic steatosis may provide a way to improve the effectiveness of exercise-based strategies in protection against MASLD.

Limitations of the study

There are some limitations in our work. First, only the role and mechanism of moderate-intensity aerobic treadmill exercise in MASLD were explored in mice in our current study. The effects of other types of exercise and exercises with different intensities on MASLD and the involvement of adipose Nrg4 in these processes remain to be explored. Second, male mice were used in our current studies. It remains to be investigated whether

adipose Nrg4 also plays an important role in exercise-mediated alleviation of MASLD in female mice.

RESOURCE AVAILABILITY

Lead contact

Requests for further information and resources should be directed to and will be fulfilled by the lead contact, Liang Guo (guoliang@sus.edu.cn).

Materials availability

This study did not generate new unique reagents. All materials generated in this study are listed in the [key resources table](#).

Data and code availability

- All data reported in this paper will be shared by the [lead contact](#) upon request.
- This paper does not report original code.
- Any additional information required to reanalyze the data reported in this paper is available from the [lead contact](#) upon request.

ACKNOWLEDGMENTS

This work was supported by The Program for Overseas High-level Talents at Shanghai Institutions of Higher Learning (TP2022100 to L.G.) and the National Natural Science Foundation of China (32070751 and 31871435 to L.G.).

AUTHOR CONTRIBUTIONS

M.C. was involved in study design, conducted the experiments, analyzed the data, and drafted the paper. Y.L., J.-Y.Z., W.-J.M., H.-Y.L., L.-J.Y., S.L., R.-Y.L., M.-T.Y., X.L., and H.-M.C. performed the experiments. L.G. conceived the idea, designed and supervised the study, obtained the funding, and co-wrote the paper.

DECLARATION OF INTERESTS

The authors declare no competing interests.

STAR★METHODS

Detailed methods are provided in the online version of this paper and include the following:

- [KEY RESOURCES TABLE](#)
- [EXPERIMENTAL MODEL AND STUDY PARTICIPANT DETAILS](#)
 - Mice
 - Cell lines
- [METHOD DETAILS](#)
 - Animals
 - Treadmill training and adeno-associated virus (AAV) treatment
 - Mouse metabolic and liver function assays
 - Primary hepatocytes isolation and cells culture
 - Lipid analysis
 - H&E staining, oil O staining
 - cGAMP levels analysis

(E) A GTT was performed in mice under 14 weeks of HFD feeding ($n = 6$ mice/group).

(F) Analysis of the GTT data in (E) with subtraction of the basal glucose to generate an AOC.

(G) An ITT was performed in mice with 15 weeks of HFD feeding ($n = 6$ mice/group).

(H) Analysis of the ITT data in (G) with AOC.

(I) and (J) Serum ALT and serum AST levels in mice, respectively ($n = 6$ mice/group).

(K) The mRNA levels of the indicated genes ($n = 6$ mice/group).

(L) The mouse liver lysates were analyzed by western blotting ($n = 3$ mice/group).

Two-way analysis of variance plus Tukey's post hoc tests were performed in (C), (D), (F), and (H)–(K). All data show the mean \pm SD. * $p < 0.05$, ** $p < 0.01$, *** $p < 0.001$.

- Chromatin immunoprecipitation (ChIP)
- Luciferase reporter assays
- Reverse transcription-quantitative PCR (RT-qPCR)
- Co-immunoprecipitation
- Detection of mice metabolic rate
- Western blotting
- Generation of recombinant adenoviruses and RNA interference
- QUANTIFICATION AND STATISTICAL ANALYSIS

SUPPLEMENTAL INFORMATION

Supplemental information can be found online at <https://doi.org/10.1016/j.celrep.2025.115251>.

Received: August 21, 2024

Revised: November 15, 2024

Accepted: January 10, 2025

Published: January 30, 2025

REFERENCES

1. Yu, C., Zhang, P., Liu, S., Niu, Y., and Fu, L. (2023). SESN2 ablation weakens exercise benefits on resilience of gut microbiota following high-fat diet consumption in mice. *Food Sci. Hum. Wellness* 12, 1961–1968. <https://doi.org/10.1016/j.fshw.2023.03.004>.
2. Yan, L., and Guo, L. (2023). Exercise-regulated white adipocyte differentiation: An insight into its role and mechanism. *J. Cell. Physiol.* 238, 1670–1692. <https://doi.org/10.1002/jcp.31056>.
3. Vetr, N.G., Gay, N.R., and MoTrPAC Study Group; and Montgomery, S.B. (2024). The impact of exercise on gene regulation in association with complex trait genetics. *Nat. Commun.* 15, 3346. <https://doi.org/10.1038/s41467-024-4596-w>.
4. Moore, T.M., Lee, S., Olsen, T., Morselli, M., Strumwasser, A.R., Lin, A.J., Zhou, Z., Abrishami, A., Garcia, S.M., Bribiesca, J., et al. (2023). Conserved multi-tissue transcriptomic adaptations to exercise training in humans and mice. *Cell Rep.* 42, 112499. <https://doi.org/10.1016/j.celrep.2023.112499>.
5. Bórquez, J.C., Díaz-Castro, F., La Fuente, F.P.d., Espinoza, K., Figueroa, A.M., Martínez-Ruiz, I., Hernández, V., López-Soldado, I., Ventura, R., Domingo, J.C., et al. (2024). Mitofusin-2 induced by exercise modifies lipid droplet-mitochondria communication, promoting fatty acid oxidation in male mice with NAFLD. *Metabolism* 152, 155765. <https://doi.org/10.1016/j.metabol.2023.155765>.
6. Guo, S., Feng, Y., Zhu, X., Zhang, X., Wang, H., Wang, R., Zhang, Q., Li, Y., Ren, Y., Gao, X., et al. (2023). Metabolic crosstalk between skeletal muscle cells and liver through IRF4-FSTL1 in nonalcoholic steatohepatitis. *Nat. Commun.* 14, 6047. <https://doi.org/10.1038/s41467-023-41832-3>.
7. Gao, Y., Hua, R., Peng, K., Yin, Y., Zeng, C., Guo, Y., Wang, Y., Li, L., Li, X., Qiu, Y., and Wang, Z. (2023). High-starchy carbohydrate diet aggravates NAFLD by increasing fatty acids influx mediated by NOX2. *Food Sci. Hum. Wellness* 12, 1081–1101. <https://doi.org/10.1016/j.fshw.2022.10.026>.
8. Zhao, Y., Zhang, R., Chen, Z., Wang, Z., Guan, S., and Lu, J. (2023). Protective effect of brain and muscle arnt-like protein-1 against ethanol-induced ferroptosis by activating Nrf2 in mice liver and HepG2 cells. *Food Sci. Hum. Wellness* 12, 2390–2407. <https://doi.org/10.1016/j.fshw.2023.03.007>.
9. Li, B.Y., Peng, W.Q., Liu, Y., Guo, L., and Tang, Q.Q. (2023). HIGD1A links SIRT1 activity to adipose browning by inhibiting the ROS/DNA damage pathway. *Cell Rep.* 42, 112731. <https://doi.org/10.1016/j.celrep.2023.112731>.
10. Luo, X., Li, Z., Chen, L., Zhang, X., Zhu, X., Wang, Z., and Chen, Y. (2023). Monocarboxylate transporter 1 in the liver modulates high-fat diet-induced obesity and hepatic steatosis in mice. *Metabolism* 143, 155537. <https://doi.org/10.1016/j.metabol.2023.155537>.
11. Luo, H.Y., Mu, W.J., Chen, M., Zhu, J.Y., Li, Y., Li, S., Yan, L.J., Li, R.Y., Yin, M.T., Li, X., et al. (2024). Hepatic Klf10-Fh1 axis promotes exercise-mediated amelioration of NASH in mice. *Metabolism* 155, 155916. <https://doi.org/10.1016/j.metabol.2024.155916>.
12. Beals, J.W., Kayser, B.D., Smith, G.I., Schweitzer, G.G., Kirbach, K., Kearney, M.L., Yoshino, J., Rahman, G., Knight, R., Patterson, B.W., and Klein, S. (2023). Dietary weight loss-induced improvements in metabolic function are enhanced by exercise in people with obesity and prediabetes. *Nat. Metab.* 5, 1221–1235. <https://doi.org/10.1038/s42255-023-00829-4>.
13. (2023). Exercise increases the metabolic benefits of weight loss. *Nat. Metab.* 5, 1084–1085. <https://doi.org/10.1038/s42255-023-00842-7>.
14. Zhu, J.Y., and Guo, L. (2024). Exercise-regulated lipolysis: Its role and mechanism in health and diseases. *J. Adv. Res.* <https://doi.org/10.1016/j.jare.2024.11.031>.
15. Chen, M., Zhu, J., Luo, H., Mu, W., and Guo, L. (2024). The journey towards physiology and pathology: Tracing the path of neuregulin 4. *Genes Dis.* 11, 687–700. <https://doi.org/10.1016/j.gendis.2023.03.021>.
16. Wang, G.X., Zhao, X.Y., Meng, Z.X., Kern, M., Dietrich, A., Chen, Z., Cozacov, Z., Zhou, D., Okunade, A.L., Su, X., et al. (2014). The brown fat-enriched secreted factor Nrg4 preserves metabolic homeostasis through attenuation of hepatic lipogenesis. *Nat. Med.* 20, 1436–1443. <https://doi.org/10.1038/nm.3713>.
17. Dai, Y.N., Zhu, J.Z., Fang, Z.Y., Zhao, D.J., Wan, X.Y., Zhu, H.T., Yu, C.H., and Li, Y.M. (2015). A case-control study: Association between serum neuregulin 4 level and non-alcoholic fatty liver disease. *Metabolism* 64, 1667–1673. <https://doi.org/10.1016/j.metabol.2015.08.013>.
18. Saeidi, A., Shishvan, S.R., Soltani, M., Tarazi, F., Doyle-Baker, P.K., Shahrbanian, S., Mollabashi, S.S., Khosravi, N., Laher, I., Moriarty, T.A., et al. (2021). Differential Effects of Exercise Programs on Neuregulin 4, Body Composition and Cardiometabolic Risk Factors in Men With Obesity. *Front. Physiol.* 12, 797574. <https://doi.org/10.3389/fphys.2021.797574>.
19. Guo, L., Zhang, P., Chen, Z., Xia, H., Li, S., Zhang, Y., Kobberup, S., Zou, W., and Lin, J.D. (2017). Hepatic neuregulin 4 signaling defines an endocrine checkpoint for steatosis-to-NASH progression. *J. Clin. Invest.* 127, 4449–4461. <https://doi.org/10.1172/jci96324>.
20. Ma, Y., Gao, M., and Liu, D. (2016). Preventing High Fat Diet-induced Obesity and Improving Insulin Sensitivity through Neuregulin 4 Gene Transfer. *Sci. Rep.* 6, 26242. <https://doi.org/10.1038/srep26242>.
21. Shi, L., Li, Y., Xu, X., Cheng, Y., Meng, B., Xu, J., Xiang, L., Zhang, J., He, K., Tong, J., et al. (2022). Brown adipose tissue-derived Nrg4 alleviates endothelial inflammation and atherosclerosis in male mice. *Nat. Metab.* 4, 1573–1590. <https://doi.org/10.1038/s42255-022-00671-0>.
22. Luo, X., Li, H., Ma, L., Zhou, J., Guo, X., Woo, S.L., Pei, Y., Knight, L.R., Deveau, M., Chen, Y., et al. (2018). Expression of STING Is Increased in Liver Tissues From Patients With NAFLD and Promotes Macrophage-Mediated Hepatic Inflammation and Fibrosis in Mice. *Gastroenterology* 155, 1971–1984.e4. <https://doi.org/10.1053/j.gastro.2018.09.010>.
23. Thomsen, M.K., Skouboe, M.K., Boulanian, C., Vernejoul, F., Lioux, T., Leknes, S.L., Berthelsen, M.F., Riedel, M., Cai, H., Joseph, J.V., et al. (2020). The cGAS-STING pathway is a therapeutic target in a preclinical model of hepatocellular carcinoma. *Oncogene* 39, 1652–1664. <https://doi.org/10.1038/s41388-019-1108-8>.
24. Verrier, E.R., Yim, S.A., Heydmann, L., El Saghire, H., Bach, C., Turon-Lagot, V., Mailly, L., Durand, S.C., Lucifora, J., Durantel, D., et al. (2018). Hepatitis B Virus Evasion From Cyclic Guanosine Monophosphate-Adenosine Monophosphate Synthase Sensing in Human Hepatocytes. *Hepatology* (Baltimore, Md) 68, 1695–1709. <https://doi.org/10.1002/hep.30054>.
25. Wang, X., Rao, H., Zhao, J., Wee, A., Li, X., Fei, R., Huang, R., Wu, C., Liu, F., and Wei, L. (2020). STING expression in monocyte-derived macrophages is associated with the progression of liver inflammation and fibrosis in patients with nonalcoholic fatty liver disease. *Lab. Invest.* 100, 542–552. <https://doi.org/10.1038/s41374-019-0342-6>.

26. Lei, Z., Deng, M., Yi, Z., Sun, Q., Shapiro, R.A., Xu, H., Li, T., Loughran, P.A., Griepentrog, J.E., Huang, H., et al. (2018). cGAS-mediated autophagy protects the liver from ischemia-reperfusion injury independently of STING. *Am. J. Physiol. Gastrointest. Liver Physiol.* 314, G655–g667. <https://doi.org/10.1152/ajpgi.00326.2017>.
27. Donne, R., Saroul-Ainama, M., Cordier, P., Hammoutene, A., Kabore, C., Stadler, M., Nemazanyi, I., Galy-Fauroux, I., Herrag, M., Riedl, T., et al. (2022). Replication stress triggered by nucleotide pool imbalance drives DNA damage and cGAS-STING pathway activation in NAFLD. *Dev. Cell* 57, 1728–1741.e6. <https://doi.org/10.1016/j.devcel.2022.06.003>.
28. Petridou, A., Tsalouhidou, S., Tsalis, G., Schulz, T., Michna, H., and Mougiou, V. (2007). Long-term exercise increases the DNA binding activity of peroxisome proliferator-activated receptor gamma in rat adipose tissue. *Metabolism* 56, 1029–1036. <https://doi.org/10.1016/j.metabol.2007.03.011>.
29. Geng, L., Liao, B., Jin, L., Huang, Z., Triggle, C.R., Ding, H., Zhang, J., Huang, Y., Lin, Z., and Xu, A. (2019). Exercise Alleviates Obesity-Induced Metabolic Dysfunction via Enhancing FGF21 Sensitivity in Adipose Tissues. *Cell Rep.* 26, 2738–2752.e4. <https://doi.org/10.1016/j.celrep.2019.02.014>.
30. Chen, M., Zhu, J.Y., Mu, W.J., Luo, H.Y., Li, Y., Li, S., Yan, L.J., Li, R.Y., and Guo, L. (2023). Cdk1-Camkk2-AMPK axis confers the protective effects of exercise against NAFLD in mice. *Nat. Commun.* 14, 8391. <https://doi.org/10.1038/s41467-023-44242-7>.
31. Zhu, J.Y., Chen, M., Mu, W.J., Luo, H.Y., and Guo, L. (2022). Higd1a facilitates exercise-mediated alleviation of fatty liver in diet-induced obese mice. *Metabolism* 134, 155241. <https://doi.org/10.1016/j.metabol.2022.155241>.
32. Bernard, J.K., McCann, S.P., Bhardwaj, V., Washington, M.K., and Frey, M.R. (2012). Neuregulin-4 is a survival factor for colon epithelial cells both in culture and *in vivo*. *J. Biol. Chem.* 287, 39850–39858. <https://doi.org/10.1074/jbc.M112.400846>.
33. Marinho, R., Ropelle, E.R., Cintra, D.E., De Souza, C.T., Da Silva, A.S.R., Bertoli, F.C., Colantonio, E., D’Almeida, V., and Pauli, J.R. (2012). Endurance exercise training increases APPL1 expression and improves insulin signaling in the hepatic tissue of diet-induced obese mice, independently of weight loss. *J. Cell. Physiol.* 227, 2917–2926. <https://doi.org/10.1002/jcp.23037>.
34. Chen, C., Jiang, C., Lin, T., Hu, Y., Wu, H., Xiang, Q., Yang, M., Wang, S., Han, X., and Tao, J. (2024). Landscape of transcriptome-wide m(6)A modification in diabetic liver reveals rewiring of PI3K-Akt signaling after physical exercise. *Acta Physiol.* 240, e14154. <https://doi.org/10.1111/apha.14154>.
35. Decout, A., Katz, J.D., Venkatraman, S., and Ablasser, A. (2021). The cGAS-STING pathway as a therapeutic target in inflammatory diseases. *Nat. Rev. Immunol.* 21, 548–569. <https://doi.org/10.1038/s41577-021-00524-z>.
36. Díaz-Sáez, F., Blanco-Sinfreu, C., Archilla-Ortega, A., Sebastian, D., Romero, M., Hernández-Alvarez, M.I., Mora, S., Testar, X., Ricart, W., Fernández-Real, J.M., et al. (2021). Neuregulin 4 Downregulation Induces Insulin Resistance in 3T3-L1 Adipocytes through Inflammation and Autophagic Degradation of GLUT4 Vesicles. *Int. J. Mol. Sci.* 22, 12960. <https://doi.org/10.3390/ijms222312960>.
37. Zhang, C., Shang, G., Gui, X., Zhang, X., Bai, X.C., and Chen, Z.J. (2019). Structural basis of STING binding with and phosphorylation by TBK1. *Nature* 567, 394–398. <https://doi.org/10.1038/s41586-019-1000-2>.
38. Chen, Q., Sun, L., and Chen, Z.J. (2016). Regulation and function of the cGAS-STING pathway of cytosolic DNA sensing. *Nat. Immunol.* 17, 1142–1149. <https://doi.org/10.1038/ni.3558>.
39. Seo, G.J., Yang, A., Tan, B., Kim, S., Liang, Q., Choi, Y., Yuan, W., Feng, P., Park, H.S., and Jung, J.U. (2015). Akt Kinase-Mediated Checkpoint of cGAS DNA Sensing Pathway. *Cell Rep.* 13, 440–449. <https://doi.org/10.1016/j.celrep.2015.09.007>.
40. (2024). Long-term exercise training has positive effects on adipose tissue in overweight or obesity. *Nat. Metab.* 6, 1657–1658. <https://doi.org/10.1038/s42255-024-01102-y>.
41. Ahn, C., Zhang, T., Yang, G., Rode, T., Varshney, P., Ghayur, S.J., Chugh, O.K., Jiang, H., and Horowitz, J.F. (2024). Years of endurance exercise training remodel abdominal subcutaneous adipose tissue in adults with overweight or obesity. *Nat. Metab.* 6, 1819–1836. <https://doi.org/10.1038/s42255-024-01103-x>.
42. Pendergrast, L.A., Ashcroft, S.P., Ehrlich, A.M., Treebak, J.T., Krook, A., Dollet, L., and Zierath, J.R. (2024). Metabolic plasticity and obesity-associated changes in diurnal postexercise metabolism in mice. *Metabolism* 155, 155834. <https://doi.org/10.1016/j.metabol.2024.155834>.
43. Zhang, L., Zou, W., Hu, Y., Wu, H., Gao, Y., Zhang, J., and Zheng, J. (2024). Voluntary wheel running ameliorated the deleterious effects of high-fat diet on glucose metabolism, gut microbiota and microbial-associated metabolites. *Food Sci. Hum. Wellness* 13, 1672–1684. <https://doi.org/10.26599/FSHW.2022.9250142>.
44. Zhang, M., Sun, W., Qian, J., and Tang, Y. (2018). Fasting exacerbates hepatic growth differentiation factor 15 to promote fatty acid β-oxidation and ketogenesis via activating XBP1 signaling in liver. *Redox Biol.* 16, 87–96. <https://doi.org/10.1016/j.redox.2018.01.013>.
45. Richter, M.M., Kemp, I.M., Heebøll, S., Winther-Sørensen, M., Kjeldsen, S.A.S., Jensen, N.J., Nybing, J.D., Linden, F.H., Høgh-Schmidt, E., Boesen, M.P., et al. (2024). Glucagon augments the secretion of FGF21 and GDF15 in MASLD by indirect mechanisms. *Metabolism* 156, 155915. <https://doi.org/10.1016/j.metabol.2024.155915>.
46. Ryu, J., Hadley, J.T., Li, Z., Dong, F., Xu, H., Xin, X., Zhang, Y., Chen, C., Li, S., Guo, X., et al. (2021). Adiponectin Alleviates Diet-Induced Inflammation in the Liver by Suppressing MCP-1 Expression and Macrophage Infiltration. *Diabetes* 70, 1303–1316. <https://doi.org/10.2337/db20-1073>.
47. Zhu, W., Sahar, N.E., Javaid, H.M.A., Pak, E.S., Liang, G., Wang, Y., Ha, H., and Huh, J.Y. (2021). Exercise-Induced Irisin Decreases Inflammation and Improves NAFLD by Competitive Binding with MD2. *Cells* 10, 3306. <https://doi.org/10.3390/cells10123306>.
48. Shi, J., Xu, W., Zheng, R., Miao, H., and Hu, Q. (2019). Neuregulin 4 attenuate tubulointerstitial fibrosis and advanced glycosylation end products accumulation in diabetic nephropathy rats via regulating TNF-R1 signaling. *Am. J. Transl. Res.* 11, 5501–5513.
49. Wang, H., Wang, L., Hu, F., Wang, P., Xie, Y., Li, F., and Guo, B. (2022). Neuregulin-4 attenuates diabetic cardiomyopathy by regulating autophagy via the AMPK/mTOR signalling pathway. *Cardiovasc. Diabetol.* 21, 205. <https://doi.org/10.1186/s12933-022-01643-0>.
50. Chen, R., Du, J., Zhu, H., and Ling, Q. (2021). The role of cGAS-STING signalling in liver diseases. *JHEP Rep.* 3, 100324. <https://doi.org/10.1016/j.jhepr.2021.100324>.
51. Sprenger, H.G., MacVicar, T., Bahat, A., Fiedler, K.U., Hermans, S., Ehrentraut, D., Riedl, K., Milenkovic, D., Bonekamp, N., Larsson, N.G., et al. (2021). Cellular pyrimidine imbalance triggers mitochondrial DNA-dependent innate immunity. *Nat. Metab.* 3, 636–650. <https://doi.org/10.1038/s42255-021-00385-9>.
52. Hildreth, A.D., Padilla, E.T., Gupta, M., Wong, Y.Y., Sun, R., Legala, A.R., and O’Sullivan, T.E. (2023). Adipose cDC1s contribute to obesity-associated inflammation through STING-dependent IL-12 production. *Nat. Metab.* 5, 2237–2252. <https://doi.org/10.1038/s42255-023-00934-4>.
53. Vila, I.K., Chamma, H., Steer, A., Saccas, M., Taffoni, C., Turtoi, E., Reinert, L.S., Hussain, S., Marines, J., Jin, L., et al. (2022). STING orchestrates the crosstalk between polyunsaturated fatty acid metabolism and inflammatory responses. *Cell Metab.* 34, 125–139.e8. <https://doi.org/10.1016/j.cmet.2021.12.007>.
54. York, A.G., Williams, K.J., Argus, J.P., Zhou, Q.D., Brar, G., Vergnes, L., Gray, E.E., Zhen, A., Wu, N.C., Yamada, D.H., et al. (2015). Limiting Cholesterol Biosynthetic Flux Spontaneously Engages Type I IFN Signaling. *Cell* 163, 1716–1729. <https://doi.org/10.1016/j.cell.2015.11.045>.

55. Qiao, J.T., Cui, C., Qing, L., Wang, L.S., He, T.Y., Yan, F., Liu, F.Q., Shen, Y.H., Hou, X.G., and Chen, L. (2018). Activation of the STING-IRF3 pathway promotes hepatocyte inflammation, apoptosis and induces metabolic disorders in nonalcoholic fatty liver disease. *Metabolism* 81, 13–24. <https://doi.org/10.1016/j.metabol.2017.09.010>.
56. Lin, Z., Yang, P., Hu, Y., Xu, H., Duan, J., He, F., Dou, K., and Wang, L. (2023). RING finger protein 13 protects against nonalcoholic steatohepatitis by targeting STING-relayed signaling pathways. *Nat. Commun.* 14, 6635. <https://doi.org/10.1038/s41467-023-42420-1>.
57. Xu, Z., Ma, Z., Zhao, X., and Zhang, B. (2024). Aerobic exercise mitigates high-fat diet-induced cardiac dysfunction, pyroptosis, and inflammation by inhibiting STING-NLRP3 signaling pathway. *Mol. Cell. Biochem.* 479, 3459–3470. <https://doi.org/10.1007/s11010-024-04950-0>.
58. Xu, D., Tian, Y., Xia, Q., and Ke, B. (2021). The cGAS-STING Pathway: Novel Perspectives in Liver Diseases. *Front. Immunol.* 12, 682736. <https://doi.org/10.3389/fimmu.2021.682736>.
59. Li, H., Hu, L., Wang, L., Wang, Y., Shao, M., Chen, Y., Wu, W., and Wang, L. (2022). Iron Activates cGAS-STING Signaling and Promotes Hepatic Inflammation. *J. Agric. Food Chem.* 70, 2211–2220. <https://doi.org/10.1021/acs.jafc.1c00681>.
60. Mao, H., Angelini, A., Li, S., Wang, G., Li, L., Patterson, C., Pi, X., and Xie, L. (2023). CRAT links cholesterol metabolism to innate immune responses in the heart. *Nat. Metab.* 5, 1382–1394. <https://doi.org/10.1038/s42255-023-00844-5>.
61. Lin, C., Kuffour, E.O., Fuchs, N.V., Gertzen, C.G.W., Kaiser, J., Hirschenberger, M., Tang, X., Xu, H.C., Michel, O., Tao, R., et al. (2023). Regulation of STING activity in DNA sensing by ISG15 modification. *Cell Rep.* 42, 113277. <https://doi.org/10.1016/j.celrep.2023.113277>.
62. Hirschenberger, M., Lepelley, A., Rupp, U., Klute, S., Hunszinger, V., Koepke, L., Merold, V., Didry-Barca, B., Wondanyi, F., Bergner, T., et al. (2023). ARF1 prevents aberrant type I interferon induction by regulating STING activation and recycling. *Nat. Commun.* 14, 6770. <https://doi.org/10.1038/s41467-023-42150-4>.
63. Liu, X., Cen, X., Wu, R., Chen, Z., Xie, Y., Wang, F., Shan, B., Zeng, L., Zhou, J., Xie, B., et al. (2023). ARIH1 activates STING-mediated T-cell activation and sensitizes tumors to immune checkpoint blockade. *Nat. Commun.* 14, 4066. <https://doi.org/10.1038/s41467-023-39920-5>.
64. Li, T., Huang, T., Du, M., Chen, X., Du, F., Ren, J., and Chen, Z.J. (2021). Phosphorylation and chromatin tethering prevent cGAS activation during mitosis. *Science* 371, eabc5386. <https://doi.org/10.1126/science.abc5386>.
65. Lu, H., Fan, L., Zhang, W., Chen, G., Xiang, A., Wang, L., Lu, Z., and Zhai, Y. (2024). The mitochondrial genome-encoded peptide MOTS-c interacts with Bcl-2 to alleviate nonalcoholic steatohepatitis progression. *Cell Rep.* 43, 113587. <https://doi.org/10.1016/j.celrep.2023.113587>.
66. Li, L., Sun, H., Chen, J., Ding, C., Yang, X., Han, H., and Sun, Q. (2023). Mitigation of non-alcoholic steatohepatitis via recombinant Orosomucoid 2, an acute phase protein modulating the Erk1/2-PPAR γ -Cd36 pathway. *Cell Rep.* 42, 112697. <https://doi.org/10.1016/j.celrep.2023.112697>.
67. Lin, Y., Yang, M., Huang, L., Yang, F., Fan, J., Qiang, Y., Chang, Y., Zhou, W., Yan, L., Xiong, J., et al. (2023). A bacteria-derived tetramerized protein ameliorates nonalcoholic steatohepatitis in mice via binding and relocating acetyl-coA carboxylase. *Cell Rep.* 42, 113453. <https://doi.org/10.1016/j.celrep.2023.113453>.
68. Ezpeleta, M., Gabel, K., Cienfuegos, S., Kalam, F., Lin, S., Pavlou, V., Song, Z., Haus, J.M., Koppe, S., Alexandria, S.J., et al. (2023). Effect of alternate day fasting combined with aerobic exercise on non-alcoholic fatty liver disease: A randomized controlled trial. *Cell Metabol.* 35, 56–70.e3. <https://doi.org/10.1016/j.cmet.2022.12.001>.
69. Petermann-Rocha, F., Wirth, M.D., Boonpor, J., Parra-Soto, S., Zhou, Z., Mathers, J.C., Livingstone, K., Forrest, E., Pell, J.P., Ho, F.K., et al. (2023). Associations between an inflammatory diet index and severe non-alcoholic fatty liver disease: a prospective study of 171,544 UK Biobank participants. *BMC Med.* 21, 123. <https://doi.org/10.1186/s12916-023-02793-y>.
70. Chen, Z., Wang, G.X., Ma, S.L., Jung, D.Y., Ha, H., Altamimi, T., Zhao, X.Y., Guo, L., Zhang, P., Hu, C.R., et al. (2017). Nrg4 promotes fuel oxidation and a healthy adipokine profile to ameliorate diet-induced metabolic disorders. *Mol. Metabol.* 6, 863–872. <https://doi.org/10.1016/j.molmet.2017.03.016>.
71. Stine, J.G., DiJoseph, K., Pattison, Z., Harrington, A., Chinchilli, V.M., Schmitz, K.H., and Loomba, R. (2023). Exercise Training Is Associated With Treatment Response in Liver Fat Content by Magnetic Resonance Imaging Independent of Clinically Significant Body Weight Loss in Patients With Nonalcoholic Fatty Liver Disease: A Systematic Review and Meta-Analysis. *Am. J. Gastroenterol.* 118, 1204–1213. <https://doi.org/10.14309/ajg.00000000000002098>.
72. Chong, B., Kong, G., Shankar, K., Chew, H.S.J., Lin, C., Goh, R., Chin, Y.H., Tan, D.J.H., Chan, K.E., Lim, W.H., et al. (2023). The global syndemic of metabolic diseases in the young adult population: A consortium of trends and projections from the Global Burden of Disease 2000–2019. *Metabolism* 141, 155402. <https://doi.org/10.1016/j.metabol.2023.155402>.
73. Zhang, H., Zhou, X.D., Shapiro, M.D., Lip, G.Y.H., Tilg, H., Valenti, L., Somers, V.K., Byrne, C.D., Targher, G., Yang, W., et al. (2024). Global burden of metabolic diseases, 1990–2021. *Metabolism* 160, 155999. <https://doi.org/10.1016/j.metabol.2024.155999>.
74. Huttasch, M., Roden, M., and Kahl, S. (2024). Obesity and MASLD: Is weight loss the (only) key to treat metabolic liver disease? *Metabolism* 157, 155937. <https://doi.org/10.1016/j.metabol.2024.155937>.
75. Zhang, Y., Fang, X., Shuang, F., and Chen, G. (2023). Dexamethasone potentiates the insulin-induced Srebp-1c expression in primary rat hepatocytes. *Food Sci. Hum. Wellness* 12, 1519–1525. <https://doi.org/10.1016/j.fshw.2023.02.019>.
76. Peng, W.Q., Xiao, G., Li, B.Y., Guo, Y.Y., Guo, L., and Tang, Q.Q. (2021). I-Theanine Activates the Browning of White Adipose Tissue Through the AMPK α -Ketoglutarate/Prdm16 Axis and Ameliorates Diet-Induced Obesity in Mice. *Diabetes* 70, 1458–1472. <https://doi.org/10.2337/db20-1210>.
77. Li, B.Y., Guo, Y.Y., Xiao, G., Guo, L., and Tang, Q.Q. (2022). SERPINA3C ameliorates adipose tissue inflammation through the Cathepsin G/Integrin/AKT pathway. *Mol. Metabol.* 61, 101500. <https://doi.org/10.1016/j.molmet.2022.101500>.
78. Guo, Y.Y., Li, B.Y., Xiao, G., Liu, Y., Guo, L., and Tang, Q.Q. (2022). Cdo1 promotes PPAR γ -mediated adipose tissue lipolysis in male mice. *Nat. Metab.* 4, 1352–1368. <https://doi.org/10.1038/s42255-022-00644-3>.
79. Huang, X., Xu, J., Xu, Y., Huangfu, B., Zhang, F., Hu, Y., Gao, R., Ren, X., Zhang, B., Huang, K., and He, X. (2024). Sulforaphane ameliorates non-alcoholic steatohepatitis by KLF4-mediated macrophage M2 polarization. *Food Sci. Hum. Wellness* 13, 2727–2740. <https://doi.org/10.26599/FSHW.2022.9250220>.
80. Zhao, H., Chen, X., Zhang, L., Meng, F., Zhou, L., Lu, Z., and Lu, Y. (2024). Lacticaseibacillus rhamnosus Fmb14 ameliorates hyperuricemia-induced hepatocyte pyroptosis via NLRP3 inflammasome cascade inhibition. *Food Sci. Hum. Wellness* 13, 2174–2186. <https://doi.org/10.26599/FSHW.2022.9250181>.
81. Sun, J., Esplugues, E., Bort, A., Cardelo, M.P., Ruz-Maldonado, I., Fernández-Tussy, P., Wong, C., Wang, H., Ojima, I., Kaczocha, M., et al. (2024). Fatty acid binding protein 5 suppression attenuates obesity-induced hepatocellular carcinoma by promoting ferroptosis and intratumoral immune rewiring. *Nat. Metab.* 6, 741–763. <https://doi.org/10.1038/s42255-024-01019-6>.

STAR★METHODS

KEY RESOURCES TABLE

REAGENT or RESOURCE	SOURCE	IDENTIFIER
Antibodies		
Total-AKT	Cell Signaling Technology	Cat# 9272S; RRID: AB_329827
phospho-AKT(S473)	Cell Signaling Technology	Cat# 4060T; RRID: AB_2315049
phospho -TBK1	Cell Signaling Technology	Cat# 5483T; RRID: AB_10693472
TBK1	Santa Cruz Biotechnology	Cat# sc-52957; RRID: AB_783995
Nrg4	ABclonal	Ca# 2599; RRID: AB_2764484
phospho -Erbb4	Santa Cruz Biotechnology	Cat# sc-81491; RRID: AB_1125702
Erbb4	ABclonal	Cat# A19047; RRID: AB_2862540
Erbb4	Santa Cruz Biotechnology	Cat# sc-8050; RRID: AB_627250
STING	Proteintech	Cat# 19851-1-AP; RRID: AB_10665370
cGAS	Proteintech	Cat# 29958-1-AP; RRID: AB_2935491
Scd1	Affinity	Cat# DF13253; RRID: AB_2846272
Flag	Proteintech	Cat# 66008-4-Ig; RRID: AB_2918475
Ppar γ	Cell Signaling Technology	Cat# 2443; RRID: AB_823598
GAPDH	Cell Signaling Technology	Cat# 5174T; RRID: AB_10622025
Peroxidase affiniPure goat anti-mouse IgG secondary antibody	Jackson	Cat# 111-035-003; AB_10015289
Peroxidase affiniPure goat anti-rabbit IgG secondary antibody	Jackson	Cat# 111-035-114; AB_2307391
Bacterial and virus strains		
Trelief® 5 α Chemically Competent Cell	Beijing Tsingke Biotech	Cat# TSC-C01-100
Chemicals, peptides, and recombinant proteins		
D-glucose	Sangon Biotech	Cat# A610219
Human insulin	Beyotime	Cat# P3376-400IU
Collagenase IV	Sigma	Cat# C5138
Oleate	Sangon Biotech	Cat# A502071
Palmitate	Sangon Biotech	Cat# A423030
Protein A/G magnetic beads	Thermo Fisher	Cat# 26162
Lipofectamine 6000	Beyotime	Cat# C0526
IP lysis buffer	Beyotime	Cat# P0013
Rosiglitazone	MedChemExpress	Cat# HY-17386
diABZI	Selleck	Cat# S8796
RU.521	MedChemExpress	Cat# HY-114180
Afatinib	Selleck	Cat# S1011
Nrg4 Protein	SinoBiological	Cat# 12183-HNCE
Critical Commercial Assays		
Triglyceride	Applygen	Cat# E1003
Cholesterol	Applygen	Cat# E1005
cGAMP	Cayman	Cat# 501700
Genomic DNA was then extracted with a PCR purification kit	Qiagen	Cat# DP203
Dual Luciferase Reporter Gene Assay Kit	Beyotime	Cat# RG027
BeyoRT™II First Strand cDNA Synthesis Kit	Beyotime	Cat# D7168M
Experimental models: Cell lines		
HEK293T	American Type Culture Collection	Cat# CRL-3216
HEK293A	China National Collection of Authenticated Cell Cultures	Cat# SCSP-5094
3T3-L1	China National Collection of Authenticated Cell Cultures	Cat# SCSP-5038

(Continued on next page)

Continued

REAGENT or RESOURCE	SOURCE	IDENTIFIER
Experimental models: Organisms/strains		
C57BL/6J	GemPharmatech	https://gempharmatech.com/
Albumin-Cre mice	the Model Animal Research Center of Nanjing University	https://www.modelorg.com/
Erbb4 ^{flox/flox}	GemPharmatech	https://gempharmatech.com/
Oligonucleotides		
Primers for real-time PCR, see Table S1	This paper	N/A
Primers for ChIP assay, see Table S1	This paper	N/A
shNC, AATTAAACCGCCAGTCAGGCT	This paper	N/A
shNrg4, GCCTGGTAGAGACAAACAATA	This paper	N/A
shPpar γ , GCCCTGGCAAAGCATTGTAT	This paper	N/A
shSTING, CAACATTGATTCCGAGATAT	This paper	N/A
shcGAS 3'UTR, CCTCTTTAGGATTGTCAGAAT	This paper	N/A
shcGAS, CTGTGGATATAATTCTGGCTT	This paper	N/A
shErbb4, CCACATAACTTCGTGGTAGAT	This paper	N/A
Recombinant DNA		
pC3.1-PPAR γ	This paper	N/A
pC3.1-Flag-cGAS-WT	This paper	N/A
pC3.1-Flag-cGAS-S291A	This paper	N/A
pC3.1-cGAS-WT	This paper	N/A
pC3.1-cGAS-S291A	This paper	N/A
Software and algorithms		
GraphPad Prism 10.1.2	GraphPad	https://www.graphpad.com/
Excel 2021	Microsoft Excel	https://www.microsoftstore.com.cn/software/office
ImageJ	ImageJ	https://imagej.nih.gov/ij/index.html
BioRender	BioRender	https://app.biorender.com/

EXPERIMENTAL MODEL AND STUDY PARTICIPANT DETAILS

Mice

All animal experiments were approved by Shanghai University of Sport Animal Care and Use Committee (Ethics No. 102772022DW001). All studies involving animal experimentation followed the National Institute of Health guidelines on the care and use of animals. Albumin-Cre mice were purchased from the Model Animal Research Center of Nanjing University. Erbb4^{flox/flox} mice were purchased from Shanghai Model Organisms Center. C57BL/6J mice were fed with high-fat diet (HFD, D12492, Research Diets) to induce hepatic steatosis, and the chow diet (CD, 1010086, Xietong Shengwu, China) was used as the control diet. All animals were housed at $23 \pm 2^\circ\text{C}$ with a humidity of $50\% \pm 5\%$ in a 12h light/dark cycle and fed *ad libitum* with standard mouse feed and water throughout the experiments.

Cell lines

Primary hepatocytes isolated from wild type male mice aged 4 to 6 weeks by using the collagenase perfusion method. The cell lines sources are as follows: HEK293T (American Type Culture Collection, CRL3216, USA), HEK293A (National Collection of Authenticated Cell Cultures, SCSP-5094, China), 3T3-L1 (National Collection of Authenticated Cell Cultures, SCSP-5038, China).

METHOD DETAILS

Animals

All animal experiments were approved by Shanghai University of Sport Animal Care and Use Committee (Ethics No. 102772022DW001). All studies involving animal experimentation followed the National Institute of Health guidelines on the care and use of animals. Albumin-Cre mice were purchased from the Model Animal Research Center of Nanjing University. Erbb4^{flox/flox} mice were purchased from GemPharmatech. Erbb4^{LKO} mice (Erbb4^{flox/flox}/Albumin Cre⁺) were generated by

crossbreeding Erbb4^{flox/flox} and albumin promoter driven Cre transgenic mice. Erbb4^{LKO} mice and their wild type (WT) littermates were used in the experiments. C57BL/6J mice were fed with high-fat diet (HFD, D12492, Research Diets) to induce hepatic steatosis, and the chow diet (CD, 1010086, Xietong Shengwu, China) was used as the control diet. All animals were housed at 23 ± 2°C with a humidity of 50% ± 5% in a 12h light/dark cycle and fed *ad libitum* with standard mouse feed and water throughout the experiments. C57BL/6J male mice were used for all the experiments.

Treadmill training and adeno-associated virus (AAV) treatment

The treadmill exercise (ZhengHuabiological, ZH-PT/5S, China) program includes 1 week of treadmill familiarization followed by 7 weeks (6 days per week) of treadmill training. During the treadmill training, we kept checking that all mice were running, but not resting, on the treadmill. This would guarantee that all mice were subjected to identical level of exercise training. The detailed treadmill programs are illustrated in the corresponding figure.

AAVs (Serotype 9) containing the shNrg4 sequence, shPpary sequence, Nrg4 coding sequence and the corresponding control vectors were packaged and purified by Genechem (Shanghai, China). Mice inguinal WAT (iWAT) pads, epididymal WAT (eWAT) pads and BAT on both sides were injected with the AAVs. The targets (5' to 3') of AAVs containing the short hairpin RNA (shRNA) were listed as follows: non-specific control shRNA (shNC), AATTAAACGCCAGTCAGGCT; shNrg4, GCCTGGTAGAGACAAA CAATA; shPpary, GCCCTGGCAAAGCATTGTAT. For AAVs delivery in iWAT, after the mice were anesthetized with isoflurane gas, longitudinal incisions were made on the skin around the inguinal areas, followed by exposure of the fat pad using tweezers. AAVs were injected into each fat pad in multiple spots (5–8 spots per fat pad). The total volume was 50 µL, and the total virus titer was 1 × 10¹¹ viral genomes (vg) for each pad (1 × 10¹¹ vg for AAV-shNC or AAV-Vector, 1 × 10¹¹ vg for AAV-shNrg4 or AAV-Nrg4). Then, the wound was rinsed with sterile saline solution and closed with a two-layer suture. For AAVs deliver in eWAT, laparotomy was performed to expose the eWAT, and the AAVs were injected as described above. For AAVs delivery in BAT, longitudinal incisions were made on the skin above the scapula to exposed of the bilateral BAT, and the AAVs were injected as described above. The detailed AAVs injection are illustrated in the corresponding figure.

Mouse metabolic and liver function assays

For GTT, the mice were fasted overnight and received an intraperitoneal (i.p.) injection of D-glucose (1.6 mg/g body weight). For ITT, the mice were injected intraperitoneally with human insulin (Eli Lilly; 0.8 mU/g body weight) after 6 h fasting. Blood glucose levels were measured at 0, 15, 30, 60, 90 and 120 min after injection (a glucometer monitor, Roche). For the GTT/ITT assays, the area of the curve (AOC) was calculated using the conventional trapezoid rule. Levels of serum alanine aminotransferase (ALT), and aspartate aminotransferase (AST) were measured using the kits from Applygen, China (#E2021 and E2023, respectively) according to the manufacturer's instructions.

Primary hepatocytes isolation and cells culture

Primary hepatocytes isolated from wild type male mice aged 4 to 6 weeks by using the collagenase perfusion method.⁷⁵ Briefly, after perfusion and digestion by collagenase IV solution (#C5138, Sigma), liver tissue was dissociated and filtered through a 70-µm cell strainer (#352350, Falcon). The resulting cell suspension was centrifuged at 50 g with 3 times to collect hepatocytes (cell pellets). Primary hepatocytes, HEK293T, and HEK293A cells maintained in Dulbecco's Modified Eagle Media (DMEM) containing 10% fetal bovine serum (FBS, Gibco) at 37°C in a 5% CO₂ environment. For 3T3-L1 preadipocyte cells differentiation, the culture medium of the 2-day post-confluent cells was replaced by DMEM containing 10% fetal bovine serum (FBS, Gibco), 1 µM dexamethasone, 2 µg/mL insulin, 0.5 mM 3-isobutyl-1-methyl-xanthine and 1 µM rosiglitazone for 48 h. Then the cells were maintained in DMEM supplemented with 10% FBS, 2 µg/mL insulin, and 1 µM rosiglitazone for another 48 h, followed by cultured in DMEM supplemented with 10% FBS for 2 days to finish differentiation process. The cell lines sources are as follows: HEK293T (American Type Culture Collection, CRL3216, USA), HEK293A (National Collection of Authenticated Cell Cultures, SCSP-5094, China), 3T3-L1 (National Collection of Authenticated Cell Cultures, SCSP-5038, China).

Lipid analysis

To establish cellular models of lipid accumulation, primary hepatocytes were seeded in six-well plates. After cell adhesion, a mixture of 0.6 mM free fatty acids (FFAs) was added to the medium for 24 h (at a final ratio of 2:1 with oleate and palmitate from Sangon Biotech, China). The cells were then fixed with 4% paraformaldehyde for 10 min and stained with Nile red and Hoechst staining for 10 min to visualize intracellular lipid accumulation. The triglyceride (TG), total cholesterol (TC) contents in isolated primary hepatocytes or liver tissue were measured using the kits from Applygen, China (#E1003 and E1005, respectively), according to the manufacturers' instructions.

H&E staining, oil O staining

The tissues were fixed in 4% paraformaldehyde and sectioned after being paraffin embedded. H&E and Oil O staining was performed as described previously^{76,77} (Olympus microscope).

cGAMP levels analysis

The cGAMP contents in liver tissue or primary hepatocytes were measured using the kits from Cayman, USA (#501700), according to the manufacturers' instructions.

Chromatin immunoprecipitation (ChIP)

ChIP was performed as described previously. Cells were cross-linked in 1% formaldehyde for 10 min at room temperature and then incubated with 125 mM glycine for termination. The cells were washed twice with ice-cold PBS, after centrifugation, resuspended in 500 µL of lysis buffer (50 mM Tris-HCl, pH 8.0, 1% SDS, 10 mM EDTA, and protease inhibitors). Samples were sonicated, and the average length of DNA fragments ranged between 200 and 800 bp. Samples were centrifuged at 12,000 g at 4°C for 5 min. After removal of an input aliquot (whole-cell extract), supernatants were diluted 10-fold in ChIP dilution buffer (20 mM Tris-HCl, pH 8.0, 150 mM NaCl, 2 mM EDTA, 1% Triton X-100, and complete protease inhibitor tablets). Then, the samples were divided equally, and 10% of each sample was used for input control. The samples were precleared using ChIP Grade Protein A/G magnetic beads (Thermo Fisher, 26162) for 1 h at 4°C and immunoprecipitated with the indicated antibodies of anti-Ppary (Cell Signaling Technology, 2443), and control IgG (Abcam, ab46540). Immunoprecipitated samples were eluted and reverse cross-linked by incubation overnight at 65°C in elution buffer (50 mM Tris-HCl, pH 8.0, 10 mM EDTA, 1% SDS). Genomic DNA was then extracted with a PCR purification kit (Qiagen). Purified DNA was subjected to qPCR using primers specific to the promoters of the indicated genes. The primers for ChIP-qPCR are listed in [Table S1](#).

Luciferase reporter assays

Luciferase reporter assays was performed as described previously.^{78,79} The proximal promoter regions of mouse Nrg4 and the artificial mutant were subcloned into the firefly luciferase reporter construct PGL3-basic (Promega). HEK293T cells were transfected with 300 ng/well firefly luciferase reporter constructs and 6 ng/well Renilla luciferase reporter plasmids, in combination with 100–300 ng/well pcDNA3.1(–) vector or Ppary plasmids, by using Lipofectamine 6000 (#C0526, Beyotime) according to the manufacturer's instructions. After 48 h, luciferase activity was measured using dual luciferase reporter assay (#RG027, Beyotime and CLARIOstar by BMG LABTECH), normalizing firefly luciferase to Renilla activity.

Reverse transcription-quantitative PCR (RT-qPCR)

Total RNA from cells and tissues was extracted by using Trizol reagent (Invitrogen) according to the manufacturer's protocol. Complementary DNA (cDNA) was synthesized from total RNA by using reverse transcription kit (Beyotime, China). The cDNAs were amplified with Power SYBR green PCR master mix (Beyotime, China), with 18S rRNA or 36b4 as an endogenous control. The results were collected from QuantStudio 6 Flex by Thermo Fisher Scientific instrument. The qPCR was done in triplicate and repeated at least 3 times. Primer information for RT-qPCR is listed in [Table S1](#).

Co-immunoprecipitation

Primary hepatocytes were lysed in IP lysis buffer (Beyotime, China). The lysate was centrifuged at 15,000 g for 10 min at 4°C, and the supernatant was collected and pre-cleaned by incubating with Protein A/G beads (Thermo Fisher, 26162) for 1 h at 4°C, then removal of Protein A/G beads. The anti-ErbB4 antibody (Santa Cruz Biotechnology, Cat: SC8055), anti-AKT (Cell Signaling Technology, Cat: 9272S) or mouse IgG (Abcam, ab46540) isotype control with the lysate for 14–16 h at 4°C. Then the samples were using Protein A/G magnetic beads (Thermo Fisher, 26162) for 4 h at 4°C. After beads were washed for 4 times with IP lysis buffer, immunoprecipitated proteins were eluted and detected by immunoblotting.

Detection of mice metabolic rate

Six-week-old mice were fed with HFD for 14 weeks. Energy expenditure was assessed using indirect calorimetry (TSE-system, XYZ, 6M/R, Germany Instruments). The concentrations of oxygen and carbon dioxide were monitored at the inlet and outlet of the sealed chambers to calculate oxygen consumption and carbon dioxide production. Each chamber was measured at an interval of 1 h.

Western blotting

Cells and tissues were harvested, prepared and western blotting was performed as described previously.^{80,81} Lysates were run on SDS-PAGE gel (BIO-RAD) and subjected to western blotting with the primary antibodies to p-AKT(S473) (Cell Signaling Technology, Cat: 9272S, Lot:28, dilution 1:1000), tAKT (Cell Signaling Technology, Cat: 4060T, Lot:25, dilution 1:1000), p-TBK1 (Cell Signaling Technology, Cat: 5483T, Lot:28, dilution 1:1000), TBK1 (Santa Cruz Biotechnology, Cat: sc-52957, Lot:J3122, dilution 1:200), Nrg4 (ABclonal, Cat: 2599, Lot: 5500009340, dilution 1:500), p-ErbB4 (Santa Cruz Biotechnology, Cat: sc-81491, Lot:B2522, dilution 1:200), Erbb4 (ABclonal, Cat: A19047, Lot:4000002639, dilution 1:800), STING(Proteintech, Cat: 19851-1-AP, Lot:00118975, dilution 1:1000), cGAS (Proteintech, Cat: 29958-1-AP, Lot:00113331, dilution 1:800), Scd1 (Affinity, Cat:DF13253, Lot:54 × 0914, dilution 1:800), Flag (Proteintech, Cat: 66008-4-Ig, Lot:10027647, dilution 1:6000), Ppary (Cell Signaling Technology, Cat: 2443, dilution 1:1000), GAPDH (Cell Signaling Technology, Cat: D16H11, Lot: 8, dilution 1:1000), peroxidase affiniPure goat anti-mouse IgG secondary antibody (Jackson, Cat: 111-035-003, Lot: 151083, dilution 1:3000); peroxidase affiniPure goat anti-rabbit IgG secondary antibody (Jackson, Cat: 111-035-003, Lot: 153526, dilution 1:3000). Western blotting was developed and quantified by using Tanon-5200S (BIO-RAD)

and ImageJ, respectively. And the values of target proteins were normalized to that of the internal control protein on the same membrane. All uncropped gels are listed in the [Data S1](#).

Generation of recombinant adenoviruses and RNA interference

The recombinant adenoviruses were performed as described previously. Recombinant adenoviruses (AD) for overexpression or knockdown were generated using ViraPower Adenoviral Expression System (Invitrogen). The short hairpin RNA (shRNA) harbored in the adenoviruses (5' to 3') were listed as follows: non-specific control shRNA (shNC), AATTTAACCGCCAGTCAGGCT; shSTING, CAACATTGATTCCGAGATAT; shcGAS 3'UTR, CCTCTTTAGGATTGTCAGAAT; shcGAS, CTGTGGATATAATTCTGGCTT; shErbb4, CCACACATAACTTCGTGGTAGAT. Recombinant adenoviruses were produced and amplified in HEK293A cells. For adenovirus infection *in vitro*, primary hepatocytes were infected with the indicated adenoviruses and replaced with fresh DMEM after 24 h of viral infection. The cells were harvested for tests 48 h after infection. For adenovirus infection *in vivo*, the indicated adenoviruses at the dose of 5×10^8 plaque-forming unites (PFU) were injected into the mice via tail vein.

QUANTIFICATION AND STATISTICAL ANALYSIS

All data showed the means \pm standard deviation (SD) of at least three biological replicates with the n indicated in each experiment. The statistical analyses were indicated in the legends of each figure, with $p < 0.05$ indicating a statistically significant difference. The statistical analysis was performed in Graphpad prism (Version 10).